PROTEINS
STRUCTURE ■ FUNCTION ■ BIOINFORMATICS

Human uroporphyrinogen III synthase: NMR-based mapping of the active site

Luis Cunha,[1,2†] Miklos Kuti,[3†] David F. Bishop,[1†] Mihaly Mezei,[3] Lei Zeng,[3] Ming-Ming Zhou,[3] and Robert J. Desnick[1*]

[1] Department of Genetics and Genomic Sciences, Mount Sinai School of Medicine, New York 10029-6574

[2] ICBAS, Instituto de Ciências Biomédicas Abel Salazar, Porto, Portugal

[3] Department of Structural and Chemical Biology, Mount Sinai School of Medicine, New York 10029-6574

ABSTRACT

Uroporphyrinogen III synthase (URO-synthase) catalyzes the cyclization and D-ring isomerization of hydroxymethylbilane (HMB) to uroporphyrinogen (URO'gen) III, the cyclic tetrapyrrole and physiologic precursor of heme, chlorophyl, and corrin. The deficient activity of human URO-synthase results in the autosomal recessive cutaneous disorder, congenital erythropoietic porphyria. Mapping of the structural determinants that specify catalysis and, potentially, protein-protein interactions is lacking. To map the active site and assess the enzyme's possible interaction in a complex with hydroxymethylbilane-synthase (HMB-synthase) and/or uroporphyrinogen-decarboxylase (URO-decarboxylase) by NMR, an efficient expression and purification procedure was developed for these cytosolic enzymes of heme biosynthesis that enabled preparation of special isotopically-labeled protein samples for NMR characterization. Using an 800 MHz instrument, assignment of the URO-synthase backbone $^{13}C_\alpha$ (100%), $^{1}H_\alpha$ (99.6%), and nonproline $^{1}H_N$ and ^{15}N resonances (94%) was achieved as well as 85% of the side-chain ^{13}C and ^{1}H resonances. NMR analyses of URO-synthase titrated with competitive inhibitors N_D-methyl-1-formylbilane (NMF-bilane) or URO'gen III, revealed resonance perturbations of specific residues lining the cleft between the two major domains of URO synthase that mapped the enzyme's active site. In silico docking of the URO-synthase crystal structure with NMF-bilane and URO'gen III was consistent with the perturbation results and provided a 3D model of the enzyme-inhibitor complex. The absence of chemical shift changes in the ^{15}N spectrum of URO-synthase mixed with the homogeneous HMB-synthase holoenzyme or URO-decarboxylase precluded occurrence of a stable cytosolic enzyme complex.

Proteins 2008; 71:855–873.

Key words: resonance assignments; chemical shift perturbation; molecular docking; enzyme complex; heme biosynthesis; porphyria.

INTRODUCTION

Uroporphyrinogen III synthase (URO-synthase[1]; hydroxymethylbilane hydrolyase [cyclizing]; EC 4.2.1.75), the fourth enzyme in the heme biosynthetic pathway, catalyzes the rapid cyclization and rearrangement of the linear tetrapyrrole, HMB, by inversion of its D-ring pyrrole to form the asymmetric cyclic tetrapyrrole and physiologic heme precursor, URO'gen III.[1] In the absence of URO-synthase, HMB rapidly and nonenzymatically cyclizes to form URO'gen I, the nonphysiologic and pathogenic isomer that accumulates in patients with congenital erythropoietic porphyria.[1] Since HMB rapidly and nonenzymatically ring-closes to form URO'gen I, the primary role of URO-synthase is to catalyze isomerization to the physiologic URO'gen III isomer. The human URO-synthase full-length cDNA and ~34 kb genomic sequence have been isolated and characterized.[2,3] The gene, located at chromosome 10q25.2-q26.3,[4] has 10 exons, and alternative promoters with tissue-specific regulatory elements for housekeeping or erythroid-specific expression.[3] Human erythrocyte and recombinant URO-synthase have been purified and characterized, and the cytosolic enzyme has been shown to function as a monomer with a molecular weight of ~29 kDa.[5,6]

Abbreviations: DTT, dithiothreitol; HMB, hydroxymethylbilane; HSQC, heteronuclear single quantum correlation; IMAC, immobilized metal affinity chromatography; IPTG, isopropyl-β-D-thiogalactopyranoside; URO-decarboxylase, uroporphyrinogen III decarboxylase; MALDI-TOF, matrix-assisted laser desorption ionization/time-of-flight; NMF-bilane, N_D-methyl-1-formylbilane; NOESY, nuclear overhauser enhancement spectroscopy; PBG, porphobilinogen; PMSF, phenylmethylsulphonyl fluoride; SUMO, small ubiquitin-related modifier; TCA, trichloroacetic acid; TCEP, tris (2-carboxyethyl) phosphine; TOCSY, total correlated spectroscopy; URO'gen, uroporphyrinogen; URO-synthase, uroporphyrinogen III synthase; Ulp1, ubiquitin-like protein.

Grant sponsor: National Institutes of Health; Grant number: 5 R01 DK026824; Grant sponsors: Portuguese Science and Technology Foundation (Programa Praxis XXI), Genetic Disease Foundation.
†Luis Cunha, Miklos Kuti, and David F. Bishop contributed equally to this work.
*Correspondence to: Robert J. Desnick, PhD, MD, Department of Genetics and Genomic Sciences, Mount Sinai School of Medicine, Fifth Avenue at 100th Street, NY 10029–6574.
E-mail: robert.desnick@mssm.edu
Received 30 April 2007; Revised 13 July 2007; Accepted 27 July 2007
Published online 14 November 2007 in Wiley InterScience (www.interscience.wiley.com).
DOI: 10.1002/prot.21755

In 1958, Bogorad first demonstrated that URO-synthase and HMB-synthase were required to synthesize URO'gen III from porphobilinogen (PBG).[7,8] Subsequently, it was hypothesized that HMB-synthase and URO-synthase, physically interacted, perhaps in a complex of the four cytosolic heme biosynthetic enzymes.[5,9,10] Experimental evidence supporting a physical protein-protein complex was provided by the PBG-induced increase in the sucrose density sedimentation rate of URO-synthase when HMB-synthase was added[10] and by the binding of URO-synthase to Sepharose-bound HMB-synthase.[9] Kinetic evidence for a close association was provided by allosterism of URO'gen III formation from PBG,[11] a decrease in the HMB-synthase K_m for PBG upon addition of URO-synthase,[12] and a decrease in the URO-synthase K_m for HMB when it was generated by coincubation with HMB-synthase instead of being added exogenously.[13] To date, however, neither the interaction of the four enzymes, nor the interaction of HMB-synthase and URO-synthase has been proven.

Recently, the crystal structure of human URO-synthase was reported at 1.85 Å resolution using a recombinant enzyme with a 21 residue N-terminal His_{10} tag extension.[14] Efforts to map the enzyme's active site and to investigate its reaction mechanism were not successful due to the inability to cocrystallize the enzyme with a substrate analogue. The active site region was inferred to be in the large cleft between the two major domains of the enzyme based on the distribution of conserved residues and by analogy to the vitamin B_{12} binding site of methionine synthase, an enzyme with partial structural homology to URO-synthase.[14] Site-directed mutagenesis of selected conserved residues did not reveal an essential catalytic residue, which suggested that "the enzymatic mechanism does not include acid/base catalysis."[14]

Here, we report the efficient and high-yield purification to homogeneity of the three cytosolic heme biosynthetic enzymes, URO-synthase, HMB-synthase, and URO-decarboxylase. Using purified isotope-labeled URO-synthase that was stable for up to 2 weeks at 30°C, we determined resonance assignments for the enzyme and demonstrated the absence of an intermolecular complex between URO-synthase and HMB-synthase or URO-decarboxylase at concentrations up to 0.3 m*M*. On the basis of NMR chemical shift perturbations of specific residues caused by interactions with the linear NMF-bilane tetrapyrrole and the cyclic tetrapyrrole reaction product, URO'gen III, the active site was mapped to specific residues in the cleft region between URO-synthase structural domains 1 and 2. In addition, *in silico* docking studies provided a model of URO'gen III binding in the mapped active site.

METHODS

Materials

Fluorescamine, porphobilinogen, leupeptin, lysozyme, and imidazole were obtained from Sigma (St Louis, MO). SuperBroth media was from Qbiogene, Inc. (Carlsbad, CA), Luria Broth (LB) from GIBCO/Invitrogen (Carlsbad, CA) and tris (2-carboxyethyl) phosphine hydrochloride (TCEP-HCl) was from Bio-Vectra DCL (Charlottetown, PEI, Canada). Factor Xa was obtained from Novagen (Madison, WI). The Bradford protein assay reagent and bovine serum albumin were purchased from Bio-Rad (Hercules, CA). All other chemicals were from Fisher Scientific (Pittsburgh, PA) except as noted.

Protein assays

Protein concentrations were routinely determined using the Bradford method according to the manufacturer's instructions. To facilitate specific activity comparisons for enzymes previously assayed by different methods, protein concentrations were also determined by the modified Lowry (*DC*™ Protein Assay, BioRad, Richmond, CA), fluorescamine,[15] and UV absorbance[16] methods, all referenced to HMB-synthase and URO-synthase solutions whose protein concentrations were determined by amino acid composition analyses performed at the Keck Molecular Analysis Laboratory, Yale University (New Haven, CT). When reporting kinetic values for the pure enzymes, the data were corrected to the amino acid composition values. The molecular mass of each purified protein was determined by matrix-assisted laser desorption ionization/time-of-flight (MALDI-TOF) mass spectrometry using a Voyager DE-STR instrument (Applied Biosystems, Foster City, CA).

URO-synthase assay

URO-synthase activity was determined as previously described for the coupled-enzyme assay[13] with the following modifications. Erythrocyte lysates containing HMB-synthase were replaced with 5 units of recombinant HMB-synthase. In addition, increased HPLC resolution of the porphyrin isomers was obtained by using a 5-μ particle size BDS Hypersil column (Thermo Electron Corp., Bellefonte, PA) equilibrated with 12% acetonitrile in 1*M* ammonium acetate, pH 5.16. Detection was enhanced using a Model 474 scanning fluorometer with excitation at 405 nm and emission at 618 nm using a gain of 100 and an attenuation of 32 (Waters, Milford, MA). One unit (U) of activity is defined as that amount of enzyme required to form one nanomole of URO III per hour at 37°C under the conditions of the assay.

HMB-synthase assay

HMB-synthase was assayed using the following modifications of our previously described method.[17] The HMB-synthase reaction mixture contained 500 μL of 0.1*M* Tris-HCl, pH 8.0 and 0.1 m*M* dithiothreitol (DTT), 200 μL of 0.5 m*M* PBG, and 50 μL of enzyme

preparation in the same buffer. Following a 30 min incubation at 37°C, the reaction was terminated by the addition of 250 μL of 50% trichloroacetic acid (TCA; wt/vol) and exposed to ~310 nm UV light for 30 min at room temperature to oxidize the porphyrinogens. The fluorescence was quantitated in an Optical Technology Devices Ratio-2 System Fluorometer (Valhalla, NY) with excitation at 405 nm using a narrow band-pass interference filter and emission at 618 nm obtained with an Optical Technology Devices 595 nm no. 2–63 sharp cut-off filter. The instrument was calibrated with 0–200 nmoles/mL of URO I Fluorescent Standard from Frontier Scientific (Logan, UT). One unit of activity is defined as that amount of enzyme required to form one nanomole of URO I per hour at 37°C.

URO-decarboxylase assay

URO-decarboxylase activity was determined as described[18] with the following modifications. HMB-synthase (6 U) and 50 μL of 2.4 m*M* PBG were incubated at 37°C in 0.1*M* Tris, pH 7.65 containing 0.1 m*M* DTT, to produce 50 μ*M* URO'gen I in 30 min. The reaction was stopped by adjusting the buffer pH to 6.8 with 0.15*M* KH_2PO_4, pH 4.5. In the dark, 300 μL of this mixture was combined with 200 μL URO-decarboxylase in 0.1*M* KH_2PO_4, pH 6.8. The reaction was incubated at 37°C for 30 min and stopped with 500 μL of 3*M* HCl. UV-mediated oxidation and HPLC separation of the decarboxylation products was as described above, except the starting gradient solutions were 50% (v/v) methanol/NaH_2PO_4, pH 4.5 and 100% methanol. One unit of activity is defined as that amount of enzyme required to form one nanomole of coproporphyrin (COPRO) I per hour at 37°C.

Human URO-synthase expression construct

This vector was engineered to include the yeast SUMO peptide, Smt3p, between the N-terminal His-Tag™ and URO-synthase. This peptide conferred increased solubility and was attached to URO-synthase via a unique cleavage site for the Smt3p-specific Ulp1 protease.[19] The yeast SUMO peptide Smt3p (nucleotides 328–621, GenBank accession number U27233), kindly provided by Dr. Troy Burke (Columbia University, NY), was inserted between the *Nhe* I and *Bam*H I sites of the pET28a N-terminal His-Tag™vector (designated pS1). The human URO-synthase cDNA encoding amino acids 1–265 (nucleotides 197–994; GenBank accession number J03824) was PCR-amplified using a forward primer that added a 5′ *Bgl* II cloning site (5′-GGAGGAAGATCTATGAAGGTTCTTT-TACTG-3′), and a reverse primer with a 3′-flanking *Sal* I site (5′-CGGCGGGTCGACTCACAGCAGCAGCAGCCA-TGGGG-3′). The URO-synthase *Bgl* II-*Sal* I insert was subcloned into the *BamH* I-*Sal* I double-digested pS1 vector, designated pSU1, and sequence confirmed in both orientations. The pSU1 plasmid was transformed into *E. coli* strain BL21-CodonPlus(DE3)-RIL-X (Stratagene, La Jolla, CA) for high-level expression. After cleavage by Ulp1, the recombinant URO-synthase was identical to wild-type enzyme plus one amino-terminal serine, for a total predicted molecular mass of 28,712 Da.

Human HMB-synthase expression construct

The human housekeeping HMB-synthase cDNA coding region (nucleotides 28–1113; GenBank accession number X04808) was PCR-amplified to add an *Nde* I restriction site at the ATG start codon using the forward primer, 5′-AGCGGAGCCCATATGTCTGGTAACGGCAAT-3′, and a *Bgl* II site was added to the 3′ end using the reverse primer, 5′-CAGAGATCTTTAATGGGCATCGTTAAGCTG-CCGTGC-3′. The PCR product was ligated into the *Nde* I/*Bam*H I-digested pET-16b expression vector (Novagen, Madison, WI) after the T7 promoter and the 5′ His-Tag to generate plasmid pH1 that was then transformed into the *E. coli* strain BL21-CodonPlus(DE3)-RIL-X as described above. The Factor Xa-cleaved recombinant enzyme was identical to the wild-type sequence with a predicted molecular mass of 39,326 Da.

Human URO-decarboxylase expression construct

The pThioHisA prokaryotic expression vector (Invitrogen, Carlsbad, CA) was modified by site-directed mutagenesis to replace the internal *Nde* I site with AGCATG, followed by a second mutagenesis step with the sequence 5′-GATGACGATGACAAGGTACCTCTGGTGCCGCGCG-GCAGCCATATGCATGAGCTCGAGATCTTC-3′ to introduce a 5′ *Nde* I cloning site and to replace the enterokinase cleavage site with a thrombin cleavage site. The human URO-decarboxylase cDNA coding region (nucleotides 109–1212; GenBank accession number NM_000374) was PCR-amplified to add 5′ *Nde* I and 3′ *Xho* I cloning sites using the forward primer 5′-CAGCTGACCCATATG-GAAGCGAATGGGTTG-3′ and reverse primer 5′-CAC-CTCGAGTCAGTTCTGTCGAAGCAGACGTGAGTGTTT-3′, digested with *Nde* I and *Xho* I, cloned into the modified pThioHis vector, designated pD1, and then transformed into *E. coli* strain Top10 (Invitrogen). The thrombin-cleaved recombinant URO-decarboxylase enzyme contained three extra amino-terminal residues (GlySerHis) and had a predicted molecular mass of 41,066 Da.

Yeast Ulp1 protease expression construct

The yeast Ulp1 protease[20] was used for cleavage of the URO-synthase/SUMO fusion peptide. The Ulp1 cDNA region encoding residues 7412 to 8071 of GenBank accession number U36624 was PCR-amplified from the *Saccharomyces cerevisiae* cosmid c9901 (ATCC, Manassas, VA) to

yield the forward and reverse sequences 5′-GGGAATTC CATATGCTGGTGCCGCGCGGCAGCCTTGTTCCTGAAT TAAATGAAAAAG-3′ and 5′-CGCCGCGGATCCTCATTT TAAAGCGTCGGTTAAAATC-3′, respectively. The PCR product was sub-cloned into the *Nde I* and *BamH I* restriction sites of the pET16b vector to generate plasmid pU1 with the protease fused to a Factor Xa-cleavable His-Tag for affinity purification. The plasmid was transformed into the host strain BL21-CodonPlus(DE3)-RIL-X (Stratagene).

Overexpression and purification of human recombinant URO-synthase

A 10-mL overnight culture in LB media containing 50 mg/mL kanamycin and the pSU1 vector in BL21-CodonPlus(DE3)-RIL was used to inoculate 1.5 L of SuperBroth (Qbiogene, Carlsbad, CA), or 2 L of M9 minimal medium (0.4% (W/V) glucose, 37.5 m*M* Na_2HPO_4, 17 m*M* KH_2PO_4, 18.7 m*M* NH_4Cl, 8.6 m*M* NaCl, 1.2 m*M* $MgSO_4$, 0.12 m*M* $CaCl_2$, and 5% thiamine in deionized water or 99.9% ^2H_2O). At A_{600} = 2 for SuperBroth or 0.7 for M9 minimal medium cultures, expression was induced with 1 m*M* isopropyl-β-D-thio-galactopyranoside (IPTG) for 4 h at 37°C, or 16 h at 20°C (SuperBroth or minimal media cultures, respectively) with shaking. All subsequent steps were preformed at 4°C. The cells were harvested at 3000*g* for 30 min. For lysis, the bacterial pellet was resuspended in 40 mL of cold buffer A (50 m*M* HEPES, pH 7.8, 0.5*M* NaCl and 5 m*M* TCEP-HCl) containing, 1 μ*M* leupeptin and 0.1 m*M* phenylmethylsulphonyl fluoride (PMSF), 330 μg/mL lysozyme (Type L7651, Sigma, St. Louis, MO), 5 μg/mL each DNase and RNase A (Sigma), and stirred gently for 30 min on ice. The suspension was freeze-thawed three times using a dry-ice/ethanol bath. The lysate was cleared by centrifugation at 35,000*g* for 30 min and then directly loaded onto a 1.6 × 7 cm immobilized metal affinity chromatography (IMAC) column containing 15 mL of (nickel) Chelating Sepharose™ Fast Flow resin (GE Healthcare, Piscataway, NJ) equilibrated with buffer A. After washing with 10 column volumes of buffer A containing 50 m*M* imidazole, the bound URO-synthase was eluted with five column volumes of buffer A containing 250 m*M* imidazole.

Prior to ion-exchange chromatography, the eluted protein was digested overnight with Ulp1 protease (1 μg/mg URO-synthase) and buffer exchanged to buffer B (50 m*M* HEPES, pH 7.0, 2 m*M* DTT) by ultrafiltration, using an Amicon Ultra 15 mL, 10,000 molcular weight cut-off, centrifugal ultrafiltration device (Millipore, Bedford, MA) according to the manufacturer's instructions. The cleaved URO-synthase preparation was loaded onto a Mono Q HR 1.0 × 10 cm ion exchange column (GE Healthcare) equilibrated with buffer B and eluted with a 240 mL gradient of 0–100% buffer B containing 200 m*M* KCl at a flow-rate of 1.0 mL/min. The peak fractions containing URO-synthase were combined, concentrated to 1 mL and exchanged to buffer C (20 m*M* sodium phosphate, pH 7.45, 150 m*M* NaCl and 2 m*M* DTT), as described above.

The concentrated post-Mono Q URO-synthase sample was fractionated into 1.0 mL aliquots from a HiLoad 1.6 × 60 cm Superdex 75 gel filtration column (GE Healthcare) equilibrated with buffer C at a flow-rate of 1.0 mL/min. The peak fractions were concentrated by ultrafiltration as described above and the buffer was exchanged to 20 m*M* sodium phosphate, pH 7.45, 100 m*M* NaCl, 2 m*M* DTT, and 0.1 m*M* EDTA as described above. For long-term storage at −80°C, 10% glycerol was added.

Overexpression and purification of human recombinant HMB-synthase

HMB-synthase was expressed and purified in three chromatographic steps as described for URO-synthase with the following modifications. Selection was with 50 μg/mL ampicillin. The IMAC eluate was adjusted to 5 m*M* $CaCl_2$ and the 21-residue His-Tag N-terminal extension was removed by digestion with 0.5 units of Factor Xa protease per mg of HMB-synthase for 2 days at 4°C. Any undigested enzyme was removed by binding the eluate to a 2 mL IMAC column equilibrated with buffer A and eluted with five column volumes of 30 m*M* imidazole in buffer A. Mono Q ion-exchange chromatography resolved the HMB-synthase isozymes with 0–3 covalently-attached PBG moieties (stable enzyme-substrate intermediates E, ES_1, ES_2, and ES_3[17]), which were further purified by gel filtration and stored as described above.

Overexpression and purification of human recombinant URO-decarboxylase

URO-decarboxylase was expressed in the Top10 host (Invitrogen), lysed from 4 L of culture, and purified as for HMB-synthase with the following modifications. The IMAC wash buffer contained 30 m*M* imidazole. The eluate was adjusted to 2.5 m*M* $CaCl_2$, and the thioredoxin N-terminal extension was removed by digestion with 1 U of thrombin protease (Novagen, Madison, WI) per mg of URO-decarboxylase eluate for 24 h at 4°C. The Mono-Q elution buffer contained 250 m*M* KCl.

Overexpression and purification of yeast recombinant Ulp1 protease

The Ulp1 protease used to cleave the Smt3p-URO-synthase fusion protein was expressed from the pU1 vector in the *E. coli* BL21-CodonPlus(DE3)-RIL host and purified in one-step using IMAC chromatography as described above. The His-Tag was not removed. About 1 μg of protease was sufficient to cleave 1 mg of

the URO-synthase fusion protein when incubated overnight in the IMAC elution buffer. Because of the fact that the Ulp1 protease recognizes a specific structure rather than a peptide sequence, it was highly specific and provided a clean product with no additional cleavages. The enzyme was stored at 1 mg/mL with addition of 10% glycerol, at −135°C, as storage at higher temperatures resulted in loss of proteolytic activity within a few months.

Physicokinetic determinations

The pH optima of purified URO-synthase and HMB-synthase were characterized over the pH range of 6.5–9.0 in 50 m*M* Bis–Tris Propane, 100 m*M* NaCl and 2 m*M* DTT, and that of URO-decarboxylase over the pH range of 5.0–8.0 in 0.2 M KH_2PO_4, 0.1 m*M* DTT. The thermostabilities of the purified enzymes were determined on aliquots of each enzyme diluted to the desired concentration (permitting direct assay without further dilution) in the same buffer used for NMR (20 m*M* NaH_2PO_4, pH 7.45, 100 m*M* NaCl, 1 m*M* EDTA, and 2 m*M* DTT) containing 1 mg/mL bovine serum albumin and incubated at 4, 30, 37, 45, and 60°C for up to 14 days. Samples were placed on ice at timed intervals, and the enzyme activities were determined at the end of the experimental time-course. The coupled-assay was used to determine the apparent K_m of recombinant URO-synthase as described by Tsai *et al.*[13] Homogeneous recombinant HMB-synthase was added in amounts yielding HMB concentrations ranging from 0.03 to 7.8 m*M*. For determining the K_m of HMB-synthase, the enzyme was diluted in 100 m*M* Tris buffer, pH 8.2, with a series of substrate concentrations ranging from 6.6 to 333 m*M*.

Isotope labeling of URO-synthase for NMR

Uniformly ^{15}N- or ^{13}C-labeled enzyme was synthesized by growing pSU1 in BL21-CodonPlus(DE3)-RIL *E. coli* in M9 minimal media containing $^{15}NH_4Cl$ (Cambridge Isotope Laboratories (CIL), Andover, MA), or U-[^{13}C]-glucose (CIL), in deionized water. $^{15}N/^{2}H$-labeled enzyme was prepared similarly in $^{2}H_2O$. After $^{15}N/^{2}H$-labeling during bacterial growth, URO-synthase was purified (as described above) in unlabeled water over the course of 1 week and then stored at 4°C for 2–4 weeks prior to NMR analysis. Uniformly $^{13}C/^{15}N/^{2}H$-labeled enzyme was prepared in a similar fashion using U-[^{13}C-^{2}H]-glucose (CIL) and 99.9% $^{2}H_2O$. Special Ile-, Val-, and Leu-labeled enzyme was prepared according to Medek *et al.*[21] and Tugarinov *et al.*[22] using $^{15}NH_4Cl$, 99.9% $^{2}H_2O$ and either 2-ketobutyric acid-1,2,3,4-$^{13}C_4$,3,3-d_2 (CIL CDLM-4611), sodium salt, 2-keto-3-methyl-d_3 butyric acid-1,2,3,4-$^{13}C_4$, sodium salt (Isotec 596418, Sigma-Aldrich, St. Louis, MS,), and [U-^{13}C-^{2}H]-glucose or 2-ketobutyric acid-4-^{13}C,3,3-d_2, sodium salt (Isotec 589276), 2-keto-3-(methyl-^{13}C)-butyric acid-4-^{13}C, 3-d_1 sodium salt (Isotec 589063), U-[^{12}C-^{2}H]-glucose (CIL), and ^{15}N-labeled, protonated Tyr and Phe (CIL).

Enzymatic synthesis of URO'gen III from porphobilinogen

URO'gen III was synthesized for the NMR perturbation studies from 1.7 μmoles of PBG (using 500 μg of purified recombinant human HMB-synthase (see above) and 100 μg of purified recombinant human URO-synthase in 13 mL of 100 m*M* Tris buffer, pH 8.2, and 2 m*M* DDT. The reaction mixture was incubated for 15 min at 37°C under nitrogen in the dark. The URO'gen III was separated from the enzymes by ultrafiltration (Amicon, 10,000 MW cut-off). The sample was then bound to 50 μL of DEAE resin (GE Healthcare), equilibrated with the reaction buffer, and eluted with 50 μL of 2*M* NaCl. The URO'gen III eluate was desalted into the NMR buffer (20 m*M* sodium phosphate, pH 7.45, 100 m*M* NaCl, 1 m*M* EDTA, and 2 m*M* perdeuterated DTT in $^{2}H_2O$) using a 10 cm × 8 mm column of Bio-Gel P-4 resin (BioRad). All buffers were degassed and bubbled with nitrogen and all procedures were performed under nitrogen in the dark using a safety light (light <600 nm blocked) to avoid oxidation of URO'gen III to URO III.

N_D-Methyl-1-formylbilane preparation

NMF-bilane octamethylester (compound 5,[23]) was kindly provided by Drs. Clotilde Pichon and Ian Scott (Texas A&M University). This compound (~1 mg) was hydrolyzed overnight with stirring in 100 μL of 2N KOH at 4°C, followed by room temperature stirring until dissolved, with protection from light. The buffer was exchanged to the URO'gen III NMR buffer as described above.

Resonance assignment and secondary structure prediction

For NMR, the proteins (typically ~0.7 m*M*) were prepared in 20 m*M* NaH_2PO_4 buffer, pH 7.45, containing 100 m*M* NaCl, 1 m*M* EDTA, 2 m*M* perdeuterated DTT, in $H_2O/^{2}H_2O$ (90%/10%) or in $^{2}H_2O$. All NMR experiments were carried out at 303 K on Bruker 800, 600 or 500 MHz spectrometers (Bruker BioSpin, Billerica, MA) equipped with a triple-resonance probe or cryoprobe, four rf channels, and pulsed field gradients. NMR data were processed and analyzed using NMRPipe[24] and NMRView.[25]

Deuterium-decoupled triple-resonance HNCACB, and HN(CO)CACB[26] spectra were recorded using U-[^{13}C,^{15}N,^{2}H]-labeled enzyme, and used to obtain backbone ($^{1}H_N$,^{15}N,$^{13}C_\alpha$ $^{13}C_\beta$) resonance assignments. 3D (H)C(CO)NH-TOtal Correlated SpectroscopY (TOCSY)[27] and

H(CCO)NH-TOCSY spectra were recorded for {I(δ1-$^{13}CH_3$),L($^{13}CH_3$,$^{12}CD_3$),V($^{13}CH_3$,$^{12}CD_3$)}-U-[^{15}N,^{13}C,^{2}H]-labeled enzyme,[22,28] and 3D ^{13}C- and, ^{15}N-edited Nuclear Overhauser Enhancement SpectroscopY (NOESY) spectra were recorded for {I(δ1-$^{13}CH_3$),L($^{13}CH_3$,$^{13}CH_3$), V($^{13}CH_3$,$^{13}CH_3$),F(^{1}H),Y(^{1}H)}-U-[^{15}N,^{2}H]-labeled enzyme.[21] These data were used to obtain valyl-methyl, leucyl-methyl and isoleucyl-δ1-methyl group carbon and proton assignments. Phenylalanine and tyrosine side-chain protons were also assigned from the above spectra combined with 2D-TOCSY and 2D-NOESY data on the same enzyme sample. The remaining side-chain resonances were assigned using a combination of 3D ^{15}N-TOCSY, ^{15}N-NOESY spectra obtained from U-[^{15}N]-labeled enzyme and 3D ^{13}C-NOESY performed with U-[^{13}C]-labeled enzyme. Stereospecific assignment of leucine and valine methyl groups was accomplished by analysis of the ^{13}C-^{13}C coupling patterns in a ^{13}C-HSQC spectrum using biosynthetically directed, fractionally (10%) ^{13}C-labeled enzyme.[29] Although the amino-terminal serine was assigned and included in the deposited data, it was excluded from residue counts here, with residue 1 being the native initiation methionine.

The CIS program of the PREDITOR web server (http://wishart.biology.ualberta.ca/shiftor/cgi-bin/preditor_current.py) was used to predict the URO-synthase secondary structure using the chemical shift index method.

In silico docking of URO'gen III and NMF-bilane to URO-synthase

The AutoDock program (version 3.05; The Scripps Research Institute, La Jolla, CA) was used to determine the lowest free energy structures for binding of URO'gen III or NMF-bilane to URO-synthase.[30] The 3D structures of each ligand were built using the InsightII program (Accelrys, Burlington, MA). The URO'gen III structure was then transferred to Charmm and energy-minimized using the Charmm27 force field parameters.[31] Two additional alternative energy-minimized ligand structures were obtained for URO'gen III by repeated "heating and cooling" of the initial structure *in silico*. The NMF-bilane structure was energy-minimized using the semi-empirical AM1 method[32] in the Gaussian-98 program[33] and only one final ligand structure was selected. For all energy-minimized ligand structures, the partial charges on individual atoms were calculated by Mulliken population analysis of the AM1 wave function. The four resulting ligand structures and the URO-synthase crystal structure coordinates (PDB ID: 1JR2-chain A[14]) were used as input to AutoDock. An initial grid of 100 × 118 × 126 points (centered on the URO-synthase molecule) with a spacing of 0.7 Å encompassed the entire molecule with sufficient space to allow the ligands to freely dock anywhere on the surface. Subsequently, a smaller grid of 94 × 72 × 84 points with a spacing of 0.375 Å was used to restrict the docking of NMF-bilane to the region of the cleft between domains 1 and 2 to increase search depth. Only the polar hydrogens were retained on the protein, all waters were removed and AutoDockTools was used to set the protein nonbonded parameters. Each docking experiment (using a genetic algorithm) consisted of an initial population of 100 individuals, 256 runs, and 5×10^6 energy evaluations per run, which yielded about 1500 generations. The remaining Autodock default settings were used. The protein structure and the cyclic tetrapyrrole methylene bridges were kept rigid, while the ligand propionic and acetic side-chains were allowed torsional flexibility. Docking results were analyzed using the program "dockres" (http://inka.mssm.edu/~mezei/dockres). The conformations with a docking free energy < -6.5 kcal/mol obtained after each multi-run experiment were clustered together based on an all-atom root mean square deviation (r.m.s.d.) tolerance of 5.0 Å. The clusters were ranked based on the docking free energy of each cluster's lowest energy conformer. The top 10 lowest energy clusters were reported.

The free energies of ligand binding estimated by Autodock are the sum of the intermolecular and ligand torsional energies calibrated empirically from actual protein-ligand dockings with known binding constants, and the K_is are calculated by Autodock using the equation: $\Delta G_{obs} = RT \ln K_i$.[30]

Resonance line broadening perturbation analyses with HMB-synthase, URO-decarboxylase, NMF-bilane, and URO'gen III

The titration experiments were carried out with 0.3 m*M* [^{15}N,^{2}H]-labeled URO-synthase (exchangeable hydrogens having been replaced with ^{1}H during the purification process) and either HMB-synthase, URO-decarboxylase, the cyclic product—URO'gen III, or the linear competitive inhibitor, NMF-bilane. Any slowly-exchangeable deuterons had already been fully replaced by protons, since no increases in signal intensities were observed for any residues during a mock titration with buffer minus ligand. Samples were in the buffer described above, and the titrations were carried out in a Bruker 500 MHz spectrometer with cryoprobe, or a Bruker 600, at 303 K. An initial [^{15}N,^{1}H]-HSQC spectrum of the free enzyme was recorded, after which ligands were added to the enzyme to obtain URO-synthase:ligand molar ratios of 4:1, 2:1, 1:1, and 1:2 (HMB-synthase); 2:1, 1:1, and 1:2 (URO-decarboxylase); 100:1, 20:1, and 10:1 (URO'gen III); 7.7:1, 4:1, and 2:1 (NMF-bilane); and 2:4:1, 1:2:1, and 1:2:2: (HMB-synthase:URO-decarboxylase), respectively, with a new spectrum recorded after each addition. Before and during analysis, the degassed samples were kept under nitrogen in the dark or under a safelight.

Resonance perturbation of URO-synthase by small molecule ligands was observed as line broadening, which results from ligand-induced conformational exchange, with a slow-intermediate exchange rate involving the ligand-bound and free forms of the enzyme that is on the same order of time scale as the NMR experiment.[34,35] To quantify the line broadening of the assigned resonances of URO-synthase perturbed by proteins and/or small molecule ligands, the intensity (peak height) of each resonance was plotted against the molar percentage of protein, URO'gen III, or NMF-bilane. The average background intensity of the spectra was subtracted from each peak intensity and then the intensities were normalized for dilution by the added ligand solution. For each residue's resonance plot, the resonance intensities (peak heights) were expressed as a percentage of the intensity with no added ligand. The percent intensity was plotted against URO'gen III concentration, and the absolute value of the slope of the least squares fit to the line was used to estimate the extent of line broadening of each residue's resonance in response to each ligand. Affected residues were divided into three groups corresponding to the extent of perturbation (strongly perturbed, red; moderately perturbed, yellow; and weakly perturbed, grey). The cut-offs between the strongly/moderately/weakly perturbed groups of residues were roughly based on the first two inflections of a plot of residue vs slope, with order of the residues being that producing a plot of continually decreasing slope values.

RESULTS

Expression and purification of human HMB-synthase, URO-synthase, URO-decarboxylase, and ulp1

The three cytoplasmic human recombinant heme biosynthetic enzymes, HMB-synthase, URO-synthase, and URO-decarboxylase, were prokaryotically expressed and milligram quantities were rapidly and efficiently purified to homogeneity using a His-Tag affinity purification strategy. Cleavage of the N-terminal His-Tag/Small Ubiquitin-related MOdifier (SUMO)/URO-synthase fusion protein with Ubiquitin-Like Protein 1 (Ulp1) protease resulted in soluble enzyme, whereas a fusion protein with an N-terminal His-Tag and a Factor Xa cleavage site was uncleavable and only partially soluble. The N-terminal His-Tag/HMB-synthase and the N-terminal thioredoxin/His-Patch/URO-decarboxylase fusion proteins were rapidly and efficiently cleaved by Factor Xa and thrombin, respectively, and then each was purified to homogeneity. SDS-PAGE showed that each enzyme was nearly pure following the initial nickel-affinity chromatographic step (see Fig. 1). Further purification by the Mono Q ion-exchange step was critical to remove most contaminating protein species, while minor contaminants were removed by a final gel filtration step.

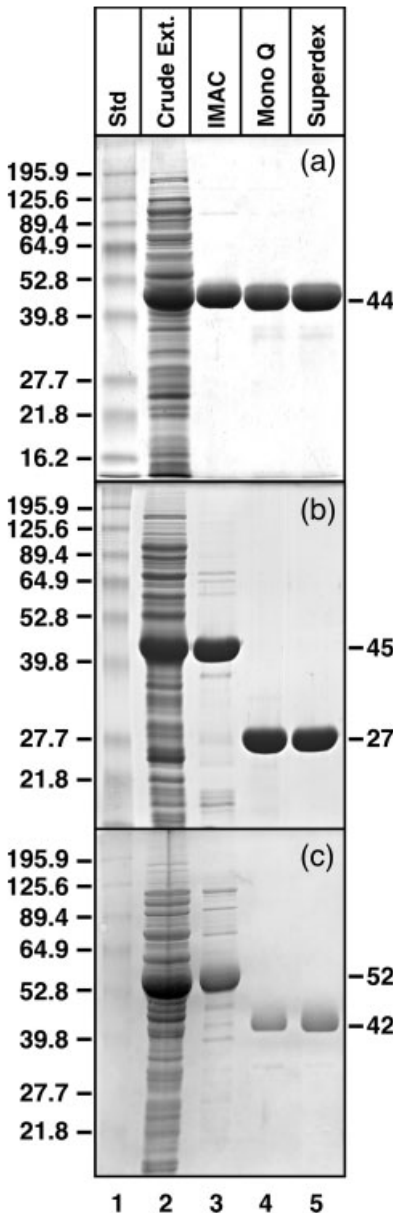

Figure 1

*SDS-PAGE of protein samples from each stage of purification. (**a**) HMB-synthase, (**b**) URO-synthase, (**c**) URO-decarboxylase. Lane 1: low molecular weight protein standards (BenchMark, GE Healthcare); lane 2: crude lysate; lane 3: IMAC eluate; lane 4: ion exchange chromatography eluate—peak fraction; lane 5: gel filtration chromatography eluate.*

As shown in Table I, a typical purification of URO-synthase resulted in >20 mg of enzyme with a specific activity of 4.3×10^6 U/mg and a 48% yield from a 1.5-L culture in SuperBroth. Similarly, the yields for purified human HMB-synthase and URO-decarboxylase were 35 and 45%, respectively. Growth of URO-synthase in minimal media

Table I
Typical Purification of Recombinant Human Heme Biosynthetic Enzymes from SuperBroth Medium

Enzyme purification step	Activity (U × 10^6)	Protein (mg)	Specific activity (U/mg)	Yield (%)
URO-synthase (1.5-L culture)				
Crude Lysate	204	600	340,000	100
IMAC	170	133	1,280,000	83
Mono Q	110	27	4,070,000	54
Superdex 70	99	23	4,300,000	48
HMB-synthase (6-L culture)				
Crude Lysate	0.765	3060	250	100
IMAC	0.642	753	852	84
Mono Q	0.281	240	1,170	37
Superdex 70	0.270	211	1,280	35
URO-decarboxylase (4-L culture)				
Crude Lysate	1.91	2,540	750	100
IMAC	1.79	544	3,290	94
Mono Q	1.02	144	7,100	53
Superdex 70	0.85	112	7,600	45

reduced the overall yield to about 30% of that from growth in SuperBroth, but the specific activities were essentially identical (data not shown).

Properties of human recombinant URO-synthase, HMB-synthase, and URO-decarboxylase

The physicokinetic properties of recombinant human enzymes were similar to those of the native erythrocyte enzymes (Table II), except for a higher URO-synthase specific activity and a somewhat higher K_m for recombinant housekeeping HMB-synthase.[5,17,36] Notably, recombinant URO-synthase had ~10-fold higher specific activity than erythrocyte enzyme, and slightly higher activity than previously reported for recombinant human URO-synthase expressed in prokaryotes[6] indicating that the recombinant enzymes had a native enzyme conformation. Several different protein determination methods were referenced to the enzyme concentration determined by amino-acid analysis to facilitate comparisons with other studies (Table II), thereby avoiding up to twofold errors of estimation. In contrast to the previously reported half-life of URO-synthase from human erythrocytes of <5 min,[5,37] the pure recombinant human enzyme had a half-life of ~5 h at 45°C at pH 8.2, the optimal pH for activity. Importantly, the recombinant human enzyme was remarkably stable at pH 7.4 ($t_{1/2}$ ~2 days at 45°C and >2 weeks at 30°C; Table II), the latter stability permitting NMR studies with high-quality spectra for residue assignments and perturbation studies. The turnover number of URO-synthase was high, 2240 min^{-1}, compared with HMB-synthase, which had a slow turnover of 1.12 min^{-1}, (Table II). HMB-synthase and URO-decarboxylase were

Table II
Physical and Kinetic Properties of Recombinant Human HMB-Synthase, URO-Synthase, and URO-Decarboxylase

Property	HMB-synthase	URO-synthase	URO-decarboxylase
M_r (Theoretical, Da)	39,742[a]	28,712	41,066
M_r (Mass Spec, Da)[b]	39,874	28,808	41,072
Protein (Bradford, mg/mL)[c]	1.54 ± 0.09	0.90 ± 0.02	1.17 ± 0.05
Protein (DC Lowry, mg/mL)[c]	1.67 ± 0.18	1.43 ± 0.09	1.23 ± 0.12
Protein (Fluram, mg/mL)[c]	0.74 ± 0.02	0.86 ± 0.01	0.62 ± 0.05
Protein (A_{280}, mg/mL)[c]	0.94 ± 0.06	1.32 ± 0.01	1.02 ± 0.01
pH Optimum	8.2	8.2	6.8
K_m (μM)	48.4	0.15	ND[d]
k_{cat} (min^{-1})	1.13	2240	ND
Catalytic efficiency ($sec^{-1}M^{-1}$)	3.9 × 10^2	2.5 × 10^8	ND
Stability at 30C, pH 7.4 ($t_{1/2}$, days)	>14	>14	>7
Stability at 45C (pH, $t_{1/2}$, days)	ND	7.4, 1.9	6.8, <<1
Stability at 60C (pH, $t_{1/2}$, min)	8.2, >120	8.2, <1	6.8, <1

[a]The calculated mass is for the apoenzyme containing the covalently bound dipyrrole cofactor.
[b]Determined for the purified enzymes by mass spectrometry.
[c]Apparent protein concentrations for a 1 mg/ml solution as determined by amino acid analysis.
[d]ND, Not determined.

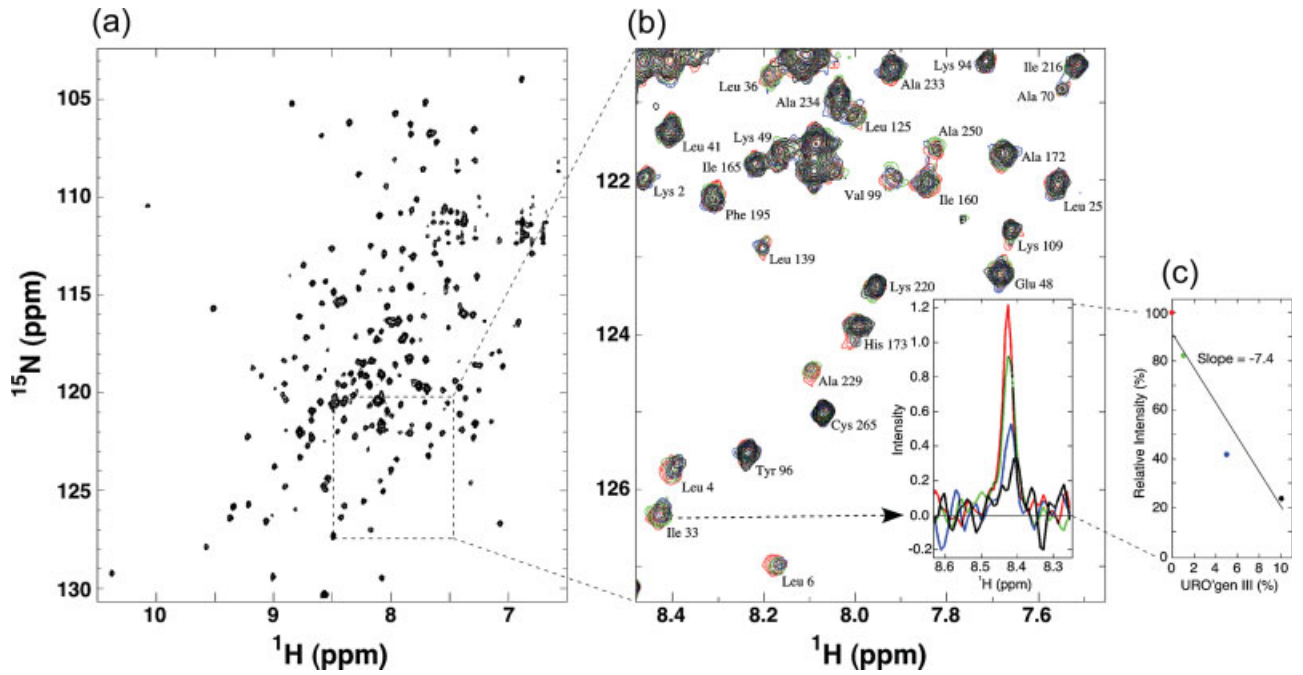

Figure 2

*Perturbation of the [^{15}N,^{1}H]-HSQC spectrum of URO-synthase by titration with URO'gen III. (**a**) Spectrum of free URO-synthase. (**b**) Detailed region of panel A overlaid with spectra collected upon titration with URO'gen III, showing the perturbation (line broadening) of URO-synthase resonances as described in Methods (red = free enzyme; green = 1% URO'gen III [molar ratio of URO'gen III:URO-synthase as a percentage; e.g., 1% = 3 μM URO'gen III]; Blue = 5%; Black = 10%). The inset shows the 1D intensity spectrum of the line-broadened I33 residue using the same color code. (**c**) Extent of line broadening estimated for residue I33 as the slope of a plot of % initial resonance intensity vs ligand % as described in Methods.*

sufficiently stable under NMR conditions for studies of their potential complex formation with URO-synthase.

Resonance assignment and data deposition

The NMR data for recombinant human URO-synthase permitted assignment of 100% of the backbone $^{13}C_{\alpha}$ resonances, 99.6% of the backbone $^{1}H_{\alpha}$ resonances and 94% of the backbone $^{1}H_{N}$ and backbone nonproline ^{15}N resonances. In addition, ~85% of the side-chain ^{13}C and ^{1}H resonances were assigned and all assignment data was deposited in the *Biological Magnetic Resonance Data Bank* (BMRB) Database (http://www.bmrb.wisc.edu), accession number 7242.[38] The only side-chain residue, for which no atoms were assigned was P198. Figure 2 shows the [^{15}N,^{1}H]-heteronuclear single quantum correlation (HSQC) spectrum of URO-synthase recorded at pH 7.45 and 303 K. The ^{13}C chemical shifts reported are referenced against the protonated enzyme, with the exception of leucine, valine methyl, and isoleucine δ-methyl shifts, that were referenced to the I(δ$^{13}CH_3$),L($^{13}CH_3$,$^{13}CH_3$), V($^{13}CH_3$,$^{13}CH_3$),F(^{1}H),Y(^{1}H)}-U-[^{15}N,^{2}H] enzyme.

The chemical shift index (CSI) method of Wishart *et al.*[39,40] was used to assign protein secondary structure by NMR. The CSI-predicted secondary structure agreed well with that calculated by DSSP[41] from the crystal structure data (see Fig. 3).

Titration of stable isotope-labeled URO-synthase with HMB-synthase or URO-decarboxylase

The URO-synthase [^{15}N,^{1}H]-HSQC spectra of [^{15}N,^{2}H]-labeled URO-synthase were recorded and compared before and after addition of HMB-synthase or URO-decarboxylase. In these experiments, the maximum URO synthase concentration was 0.3 m*M* and that of HMB synthase or URO decarboxylase was 0.4 m*M*. The deuteration level achieved using 99.9% D_2O without deutero-glucose was sufficient for the titrations since no significant spectral differences were detectable between [^{15}N]-HSQC spectra collected with this sample and one prepared with 100% deuteration. The HMB-synthase isoform used in this titration was the "A" form[17] holoenzyme containing only the covalently-bound dipyrromethane cofactor.[42] As shown for one region of the spectrum in Figure 4, only the resonance for residue N77 was minimally perturbed when URO-synthase was titrated with HMB-synthase [Fig. 4(a); in the rest of the spectrum,Y19, T62, and A222 were also very slightly perturbed]. When titrated with URO-decarboxylase, only resonances for residues E48, and S212 were

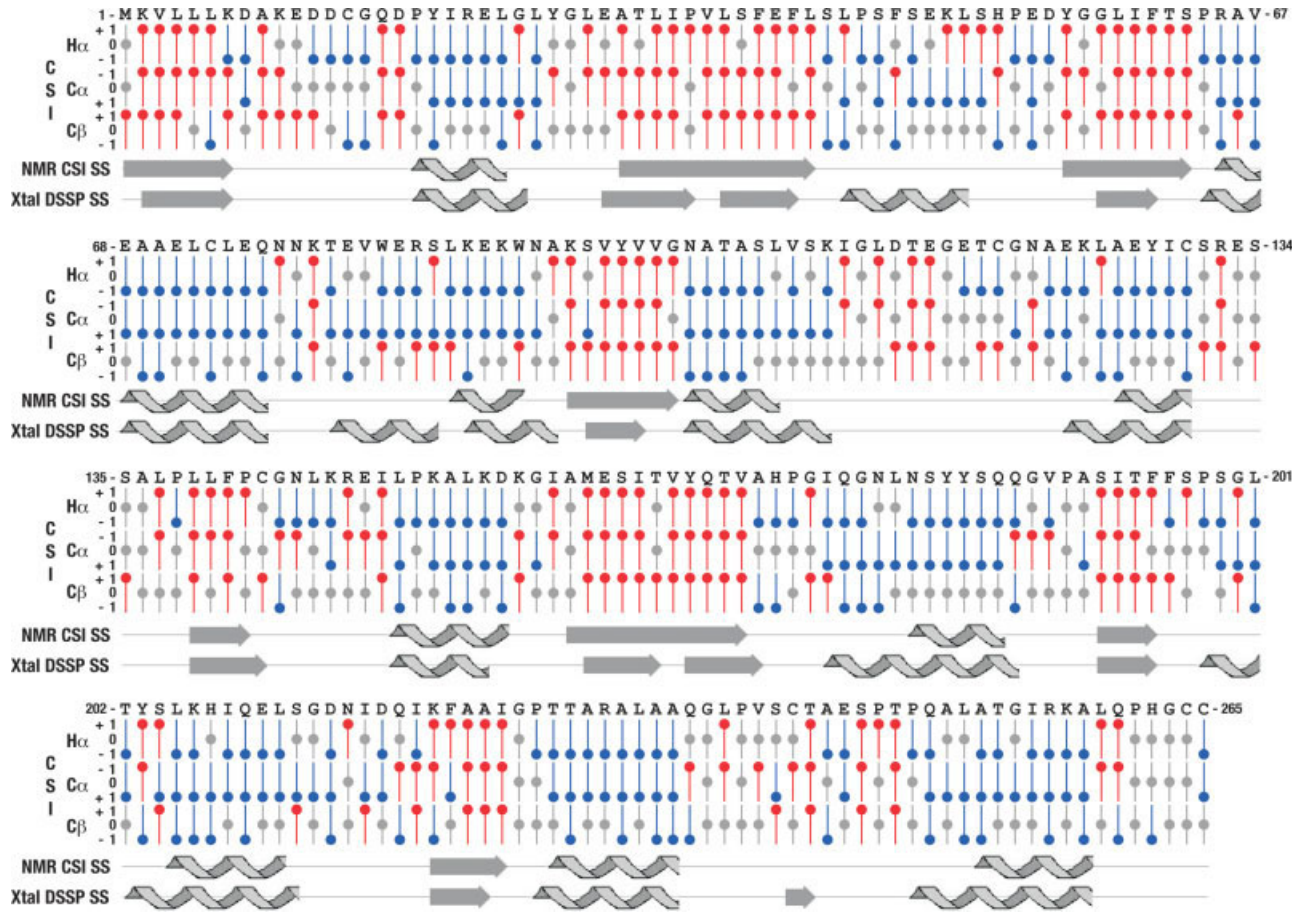

Figure 3

CSI prediction of the secondary structure of URO-synthase. The CSI determined by the PREDITOR program for Hα, Cα, and Cβ resonances are plotted under the URO-synthase amino acid sequence and the predicted secondary structures are indicated with arrows for beta structures and helices for α-helix structures. For comparison, the published secondary structure[14] calculated by DSSP (Xtal DSSP SS) for the crystal structure is shown below the CSI secondary structure prediction (NMR CSI SS). The results are displayed in a format similar to that used by the NMRview program. Note that the CSI values for Cαs were plotted in the opposite orientation to those for Hα and Cβ to make it easier interpret the structure predictions. [Color figure can be viewed in the online issue, which is available at www.interscience.wiley.com.]

slightly perturbed [Fig. 4(b)]. These weak perturbations that did not cluster together were presumably artifacts due to slight differences in pH or ionic strength between the URO-synthase and added enzyme. Thus, these results did not support a stable interaction between URO-synthase and the adjacent cytosolic heme biosynthetic enzymes, HMB-synthase and URO-decarboxylase.

When URO-synthase was titrated with individually-purified HMB-synthase enzyme-substrate intermediates "B" through "D" containing one (ES1) to three (ES3) additional pyrrole units, increasingly strong resonance perturbations were observed as chain length increased (data not shown). However, it was noted that the URO'-gen III formed during the experiment was sufficient to account for these perturbations. This URO'gen III was generated from substrate-loaded HMB-synthase by catalytic conversion of the released HMB by URO-synthase.[43] Essentially identical URO-synthase perturbation results were obtained when the same low concentration of URO'gen III (~15 μ*M*) was incubated with URO-synthase in the absence of HMB-synthase (e.g., see NMR perturbation mapping studies below).

When URO-decarboxylase was titrated into a 1:2 mixture of URO-synthase:HMB-synthase (mix of forms A-D), no significant perturbation of the URO-synthase HSQC spectrum was seen, indicating the absence of a ternary complex of these cytosolic heme biosynthetic enzymes (data not shown).

Mapping of the URO-synthase active site by NMR perturbation studies

To experimentally map the active site, chemical shift perturbation studies were performed by titrating

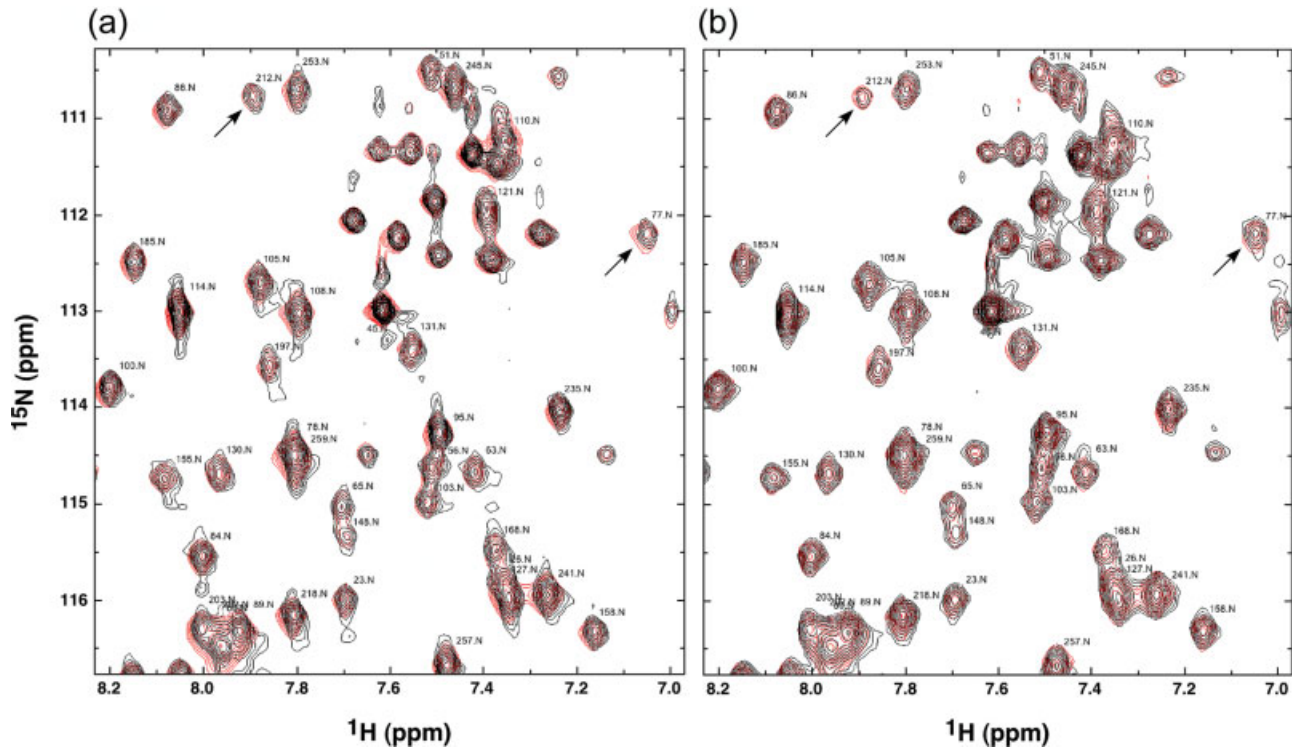

Figure 4

*[^{15}N,^{1}H]-HSQC spectra of labeled URO-synthase mixed with the prior or subsequent enzyme in the pathway. (**a**) [^{15}N,^{1}H]-URO-synthase (resonances shown in red) was titrated with increasing concentrations of HMB-synthase (shown in black overlay for the 1:1 mixture) as described in methods. For the region of the spectrum shown, only N77 was slightly line-broadened at the highest concentration (0.3 mM) of added enzyme. (**b**) Titration with URO-decarboxylase as in (a), with the 1:1 mixture with URO-decarboxylase in black overlay; only S212 was slightly line-broadened at the highest enzyme concentration (0.3 mM). Arrows identify the resonances of residues 77 and 212.*

[^{15}N,^{2}H]-labeled URO-synthase with unlabeled URO'gen III or NMF-bilane in 10% D_2O/90% H_2O. These studies revealed that specific assigned backbone resonances in the [^{15}N,^{1}H]-HSQC spectrum underwent line broadening in a ligand-concentration dependent manner, indicating a slow to intermediate exchange rate. The changes in peak intensities were determined as a measure of line broadening to map the ligand binding sites on the protein. An overlay of a region of unperturbed and increasingly perturbed URO-synthase [^{15}N,^{1}H]-HSQC spectra (with titration by URO'gen III) is shown in Figure 2(b). To quantitate the extent of perturbation, the slopes of peak intensity versus ligand concentration [Fig. 2(c)] for each resonance were plotted [Fig. 5(a,b)]. Of the 235 assigned resonances, 194 could be monitored for changes in peak intensities, the remaining 41 overlapped with each other or were too weak to quantitate. Titration with URO'gen III induced line broadening in 88 resonances and NMF-bilane titration resulted in 94 line-broadened resonances.

The residues most strongly perturbed by URO'gen III involved 18 backbone resonances in the [^{15}N,^{1}H]-HSQC spectrum [Fig. 5(a)]. These residues included L6, K7, D8, I33, V35, L36, T62, S63, R65, G100, T103, R148, L151, F196, S197, G200, A229, and L251. Of these, L6, K7, I33, L36, T62, S63, R65, G100, T103, F196, S197, G200, and L251 were highly conserved (92–100% identity in 13 eukaryotes (data not shown). The locations of these 18 most strongly perturbed residues in the URO-synthase 3D crystal structure [PBD code 1JR2, Chain A[14]] are indicated in red in Figure 6. The strongly perturbed resonances were all from residues at or near the surface forming the major crevice between the two globular domains of the enzyme, and thus, map the active site. Additional residues in the interior and hinge regions of the enzyme showed moderate line broadening upon ligand binding [Figs. 5(a) and 6, indicated in yellow], presumably due to conformational change of the enzyme. Consistent with the previous suggestion that the protein is flexible and able to adjust its inter-domain distance,[14] movement about a hinge region would allow the two domains to approach each other without requiring major changes in their individual conformations. Of note, most of the strongly perturbed residues occurred in clusters that contained other adjacent strongly and/or moderately perturbed residues (see Fig. 5).

Similarly, perturbation titrations were conducted using the linear substrate analogue, NMF-bilane. This inhibitor

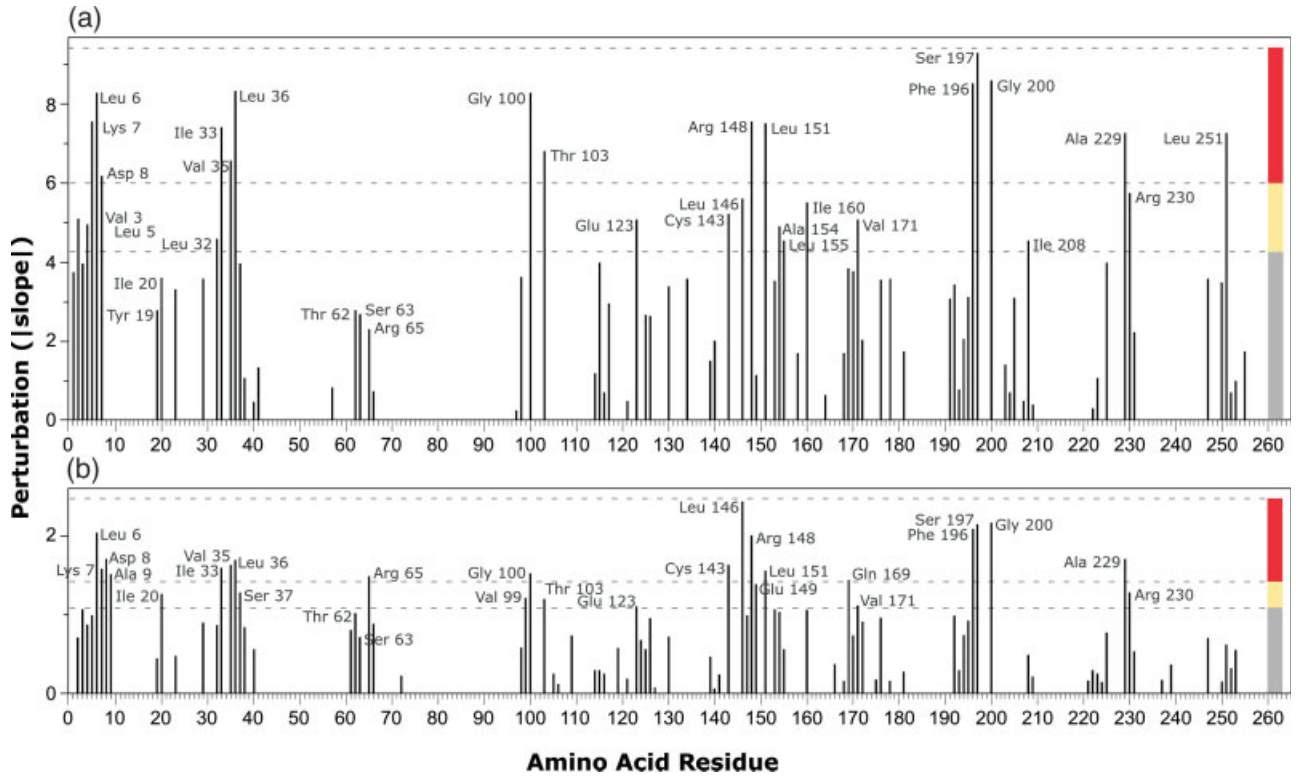

Figure 5

*Perturbation of URO-synthase resonance intensities by (**a**) URO'gen III and (**b**) NMF-bilane. The absolute values of the slopes of the intensity vs percent ligand plots describe the extent of line broadening and were calculated as described in Methods and as shown in Figure 2. The most strongly perturbed residues were between the slope values indicated by the red bar, while moderately perturbed residues were defined by the yellow bar boundaries. Weakly perturbed residues are demarcated by the grey bar. [Color figure can be viewed in the online issue, which is available at www.interscience.wiley.com.]*

strongly perturbed the same residues that were strongly perturbed by URO'gen III, except for T103 (moderately perturbed) and L251 (weakly perturbed) [Fig. 5(b)]. Approximately 10 times more NMF-bilane was required to give similar extents of perturbation (50% NMF-bilane was equivalent to 5% URO'gen III). Notably, the clusters of adjacent perturbed residues were nearly identical for both URO'gen III and NMF-bilane [comparing Fig. 5(a,b)], the main differences being the relative intensities of individual cluster members. Although the peak intensities for the clusters that included Y19, I20, and R65 were lower than the yellow-coded cut-off values in Figure 5(a), they were yellow-coded in Figure 6 since they represented unique clusters and were significantly perturbed by NMF-bilane. Of these, Y19 and R65 were highly conserved in eukaryotes. Some differences in relative perturbation intensities caused by the closed-ring URO'gen III and the linear NMB-bilane ligands were observed, possibly due to their structural differences. Residues, which were more perturbed by URO'gen III were L151, V171, I208, and L251, while those more perturbed by NMF-bilane were A9, R65, L146, and Q169.

Modeling of the URO-synthase active site by *in silico* docking

In silico docking to the crystal structure of human URO-synthase[14] (PDB: 1JR2, Chain A) was performed using three alternative energy-minimized structures for URO'gen III [Fig. 7(a)] and one for the linear tetrapyrrole, NMF-bilane [Fig. 7(b)] both competitive inhibitors of substrate binding.[23,45] Each structure was used in separate docking experiments, which held the protein and the cyclic tetrapyrrole bridge methylenes in a rigid conformation, while allowing conformational change of the ligand side-chains to robustly assess local possibilities for energy minimization of ligand binding. The lowest energy clusters for all three URO'gen III structures docked in the cleft between URO-synthase domains 1 and 2 and the best three were centered above D8, with ring D left of the hinge β-sheets, closest to residue R148. [Fig. 8(a)]. The cluster with the most conformers (68 members) was the "top ranking" cluster whose lowest energy conformer had a $\Delta G_{docking} = -16$ kcal/mol, a $\Delta G_{binding} = -7.2$ kcal/mol, a predicted binding constant (K_i) of 5.7 μ*M*, and fit

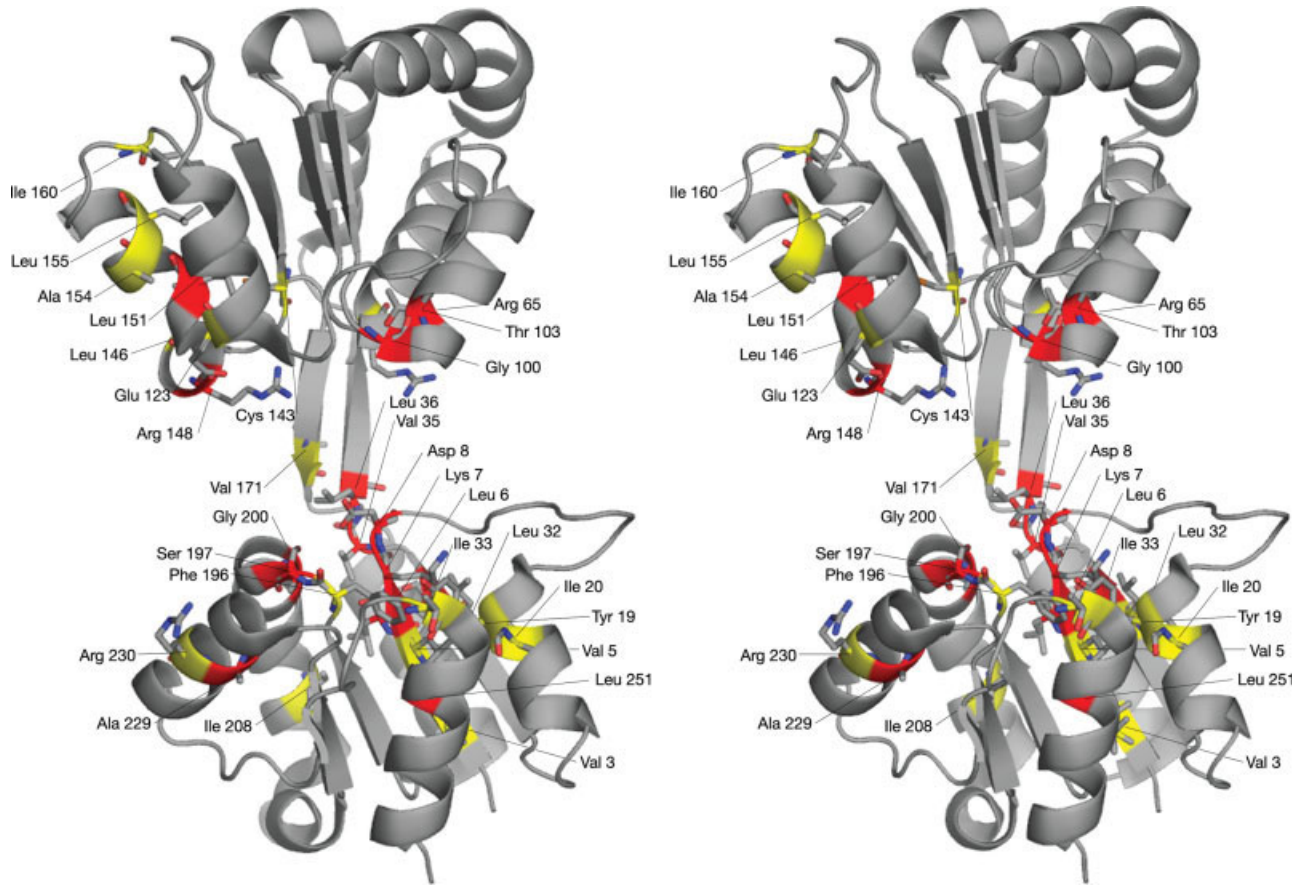

Figure 6

*Stereogram of the crystal structure of URO-synthase showing the residues that were moderately to strongly perturbed during titration with (**a**) URO'gen III or (**b**) NMF-bilane. The α carbon color was assigned as in Figure 5. This figure, as well as Figures 7, 8, 9, and 10 was generated with the molecular visualization program, Pymol.*[53]

tightly into the domain 1 interface of the cleft (see Fig. 9). By comparison, the second and third best clusters had only seven and one members, respectively. Docking analyses using the B-chain from the crystal structure did not provide as well-clustered results, consistent with the suggestion that alternative conformations of the enzyme may promote product release.[14]

Although most of the enzyme's surface was negatively-charged, the cleft region occupied by the negatively-charged ligand was largely positive. Residues with one or more atoms within 4 Å of this URO'gen III conformer included D8, centered below the hydrogens on the tetrapyrrole nitrogens, E11 and Y19 near the tetrapyrrole B-ring propionate, A9, S37, and F38 near the A-ring propionate, L36 near the methylene bridge between rings A and D, R65 and T170 near the A-ring acetate, R148 and T170 near the D-ring acetate, F196, T227 and T228 near the C-ring propionate, S197 and S199 near the D-ring propionate, and P246 near the C ring acetate.

Likewise, the energy-minimized NMF-bilane structure with fixed torsions of the A to C ring methylene bridges docked with its top 10 clusters in positions similar to those of URO'gen III [Fig. 8(b)]. Most clusters were nearly congruent with the position of the best URO'gen III conformer, but rotated clockwise (looking down from the upper domain 2) one pyrrole unit. Although the three top-ranked clusters had only 12, 7, and 6 members each respectively, the fourth top-ranked cluster had 66 members. The $\Delta G_{docking}$ of the best conformer of the fourth cluster was -15 kcal/mol and the $\Delta G_{binding}$ was -4.6 kcal/mol corresponding to a predicted K_i of 400 μM (about 100-fold weaker than that predicted for the best URO'gen III conformer). Residues within 4 Å of these two conformers included the same residues as found for URO'gen III docking except for absent S37 and F38 contacts and added contacts K7 near the A-ring propionate, T62 and P64 near the D-ring propionate, S63 and Y168 near the C-ring propionate, and G200

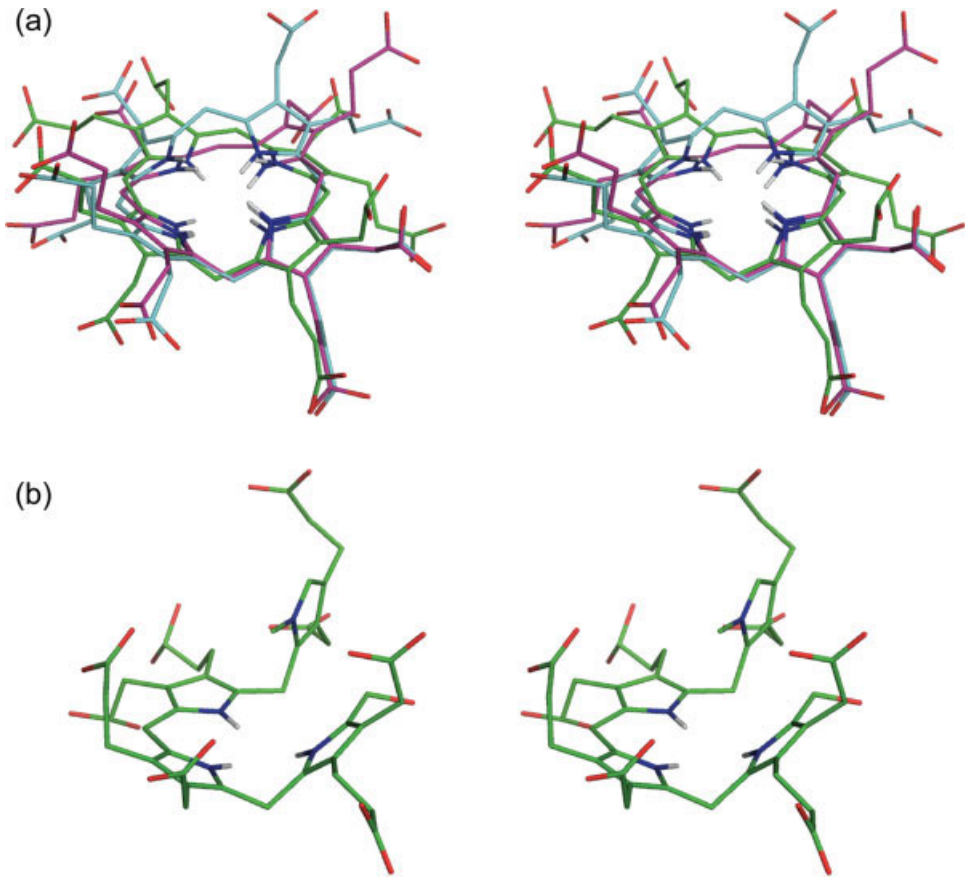

Figure 7

*Energy minimized structures used as input for Autodock. (**a**) Three alternative conformers of URO'gen III (see Materials and Methods); (**b**) NMF-bilane. [Color figure can be viewed in the online issue, which is available at www.interscience.wiley.com.]*

near the B-ring propionate. Thus, the docking results for both the URO'gen III and NMF-bilane supported the location of the center of the tetrapyrrole ring directly above aspartate 8 with the peripheral acid groups contacting both domain 1 and 2 residues lining the surface of the cleft between the domains.

Notably, the docking results (based on the 3D crystal structure of URO-synthase) for the lowest energy URO'gen III conformer coincided with the URO'gen III perturbation results, which mapped the active site to a specific cleft region between domains 1 and 2 (see Fig. 10). Note that of the 18 most strongly perturbed residues, 12 (K7, D8, Y19, L36, T62, S63, R65, G100, T103, R148, F196, and S197) form surfaces directly above or below the Autodock-predicted location of URO'gen III binding. The domain 1 surface and the domain 2 surface formed by R148 and R65, are in close proximity to the ligand while the domain 2 surface formed by T62, S63, G100, and T103 is more distant from the ligand in the crystal structure. Therefore, the NMR perturbation data predicts that the solution structure of the active site region is more closed than the crystal structure shown in Figure 10. Contacts were also predicted but could not be analyzed for unassigned (or unassignable) residues (P64, P198), S199, T227, T228, and (P246). Thus, the *in silico* docking studies confirmed the NMR perturbation results, which mapped the location of the URO-synthase active site.

Intermolecular NOEs between the NMF-bilane inhibitor and the reverse labeled $^{13}C/^{1}H$-methyl protons of valine and leucine, and the $^{13}C/^{1}H$-δ-methyl isoleucine protons of otherwise deuterated URO-synthase were evaluated for confirmation of the results of the resonance perturbation studies. Unfortunately, of the 63 methyl-labeled residues, only one (L36) was predicted to be within 5 Å of the carbon-attached protons of the inhibitor in the *in silico* docking studies (data not shown). However, no NOE was observed for this residue. Future NMR solution-structure studies may clarify this finding.

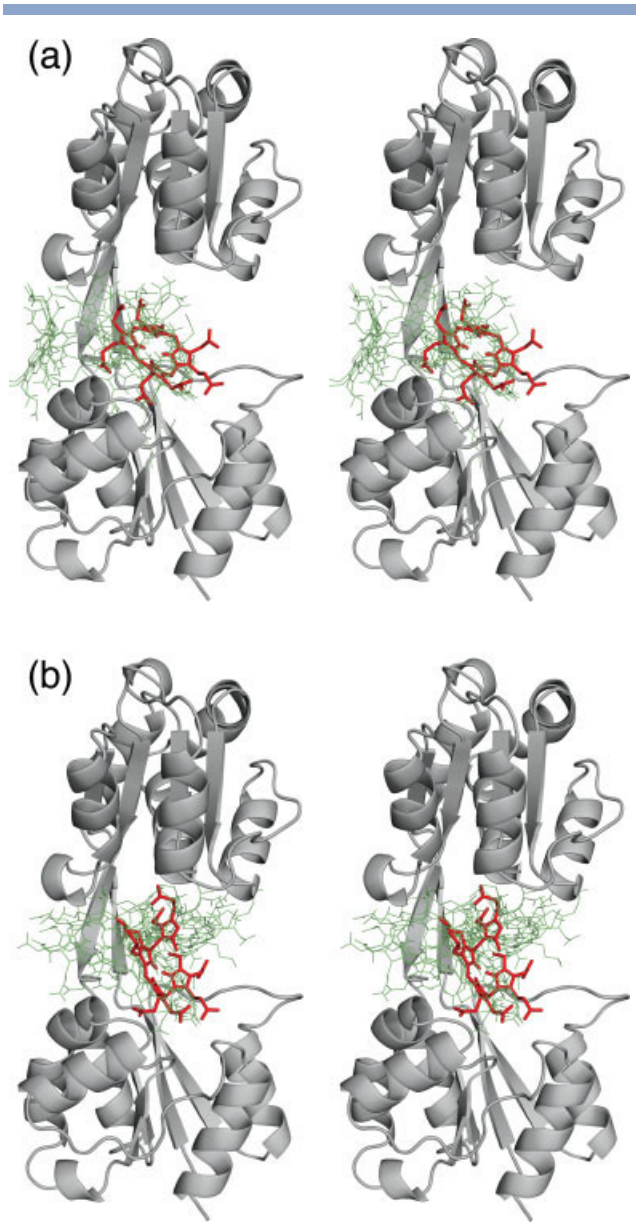

Figure 8

*Crystal structure model of URO-synthase docked with ligands. The energy minimized ligands were docked to the crystal structure[14] of URO-synthase (see Materials and Methods). Each cluster of docked ligands was ranked based on the lowest energy conformer in each cluster. (**a**) The lowest energy conformer from each of the top 10 clusters for the three URO'gen III conformers are shown. The lowest energy representative from the top-ranked cluster is highlighted by an increase in bond thickness, and is colored red; (**b**) The lowest energy conformer from each of the top 10 clusters for the NMF-bilane conformer are shown. The* $\Delta G_{docking} = -15$ *kcal/mol conformer mentioned in "Results" is highlighted in red. [Color figure can be viewed in the online issue, which is available at www.interscience.wiley.com.]*

DISCUSSION

NMR studies of recombinant human URO-synthase were undertaken to determine its backbone and side-chain resonance assignments, to map its active site in solution, and to investigate the possible interaction of the cytosolic heme biosynthetic enzymes in a biosynthetic complex or "metabolon." For these studies, milligram quantities of recombinant human HMB-synthase, URO-synthase, and URO-decarboxylase were expressed and purified. For each enzyme, the choice of fusion peptide was critical and unique for the efficient expression of soluble and stable recombinant activity. The HMB-synthase His-Tag fusion protein was cleavable with Factor Xa, however, the His-Tag URO-synthase fusion in pET16b was not (data not shown). In fact, the recombinant enzyme used to solve the crystal structure of URO-synthase included a 21-residue His-Tag.[14] In contrast, the N-terminal His-Tag-SUMO fusion protein used here for NMR studies was specifically cleavable by the small Ulp1 protease, leaving only a single N-terminal serine residue, and provided much larger quantities of soluble enzyme than a previous recombinant method.[6] Importantly, recombinant human URO-synthase was stable at pH 7.45 for over 2 weeks at 30°C, which was required for the NMR studies. For URO-decarboxylase, a thrombin cleavable His-Tag/thioredoxin fusion protein provided highly purified and soluble enzyme. The physicokinetic properties of these enzymes were comparable with those of their native counterparts, with the notable exception of the significantly higher specific activity for recombinant URO-synthase and a higher K_m value for recombinant housekeeping HMB-synthase (Table II).

Although the ~29 kDa human URO-synthase was relatively large for NMR structural analysis, the complete assignment of all backbone carbons, all but one backbone alpha hydrogen, 94% of the backbone $^{1}H_N$ and backbone nonproline ^{15}N resonances, and 85% of the nonproline side-chain resonances (BMRB accession number 7242) was achieved by use of an 800 MHz NMR spectrometer with a cryoprobe. The URO-synthase backbone resonance assignments permitted mapping of the enzyme's active site by 2D [^{15}N,^{1}H]-HSQC resonance perturbation studies using the competitive inhibitors URO'gen III and NMF-bilane, and studies of potential protein-protein interactions between URO-synthase and HMB-synthase or URO-decarboxylase.

Previous physical and kinetic evidence suggested that HMB-synthase and URO-synthase were physically interactive in a complex, and possibly, that the four cytosolic heme biosynthetic enzymes were efficiently organized in an enzyme complex or metabolon.[5,9–12] However, our NMR perturbation studies did not find evidence for complex formation when URO-synthase was incubated with equimolar concentrations of either holo-HMB-synthase (the "A," or "ES" form containing only the dipyrrole cofactor) or URO-decarboxylase (see Fig. 4), or with enzyme-substrate intermediates B through D. Furthermore, there was no evidence of a ternary complex. Thus, these NMR studies did not support the occurrence of a URO-synthase complex with HMB-synthase and/or

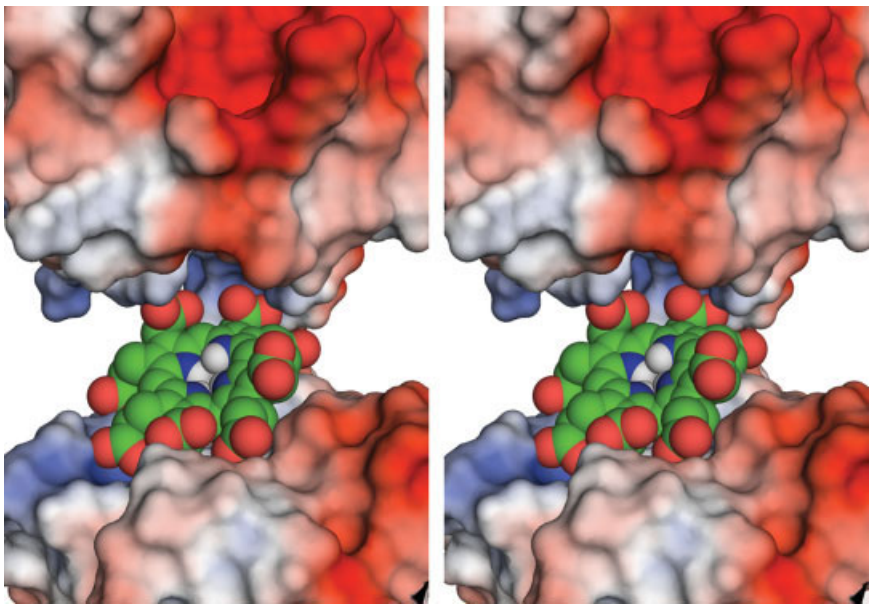

Figure 9

Stereogram of the complex between URO-synthase and the lowest energy docked URO'gen conformer. The URO-synthase surface was colored according to its electrostatic potential, ranging from −4 kT/e (red) to +4 kT/e (blue), calculated with the computer program APBS tools.[54] The docked URO'gen conformer was represented as spheres (atom colors: C = green, O = red, N = blue, H = white).

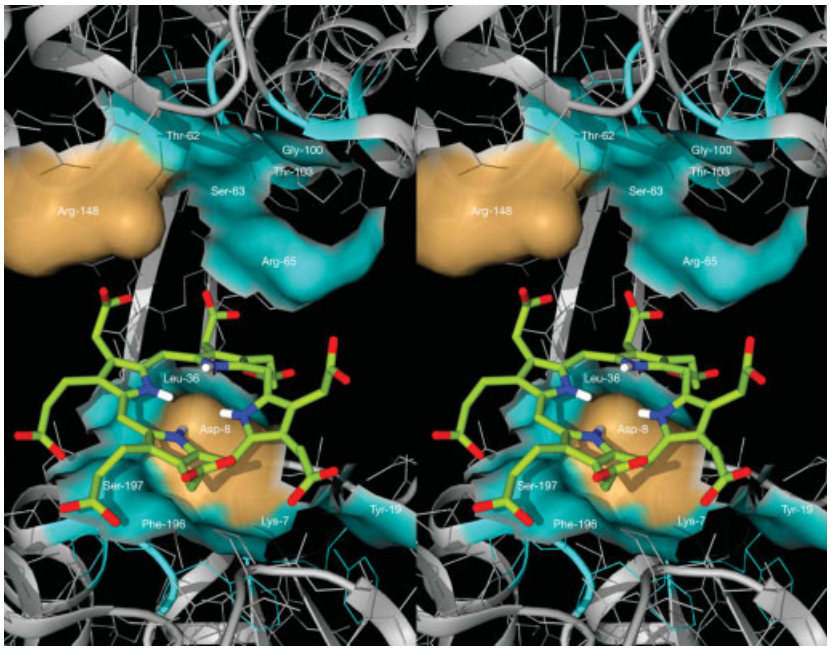

Figure 10

Mapping of the URO-synthase active site. The cleft region between domains 1 and 2 of the 3D crystal structure is shown in stereo, highlighting the surfaces formed in the cleft between domains 1 and 2 by residues whose NMR resonances were highly-perturbed by URO'gen III binding. The surfaces for residues exhibiting 92–100% sequence identity in 13 eukaryotes are teal colored and residues with 54 to 62% identity are sand-colored.

URO-decarboxylase. It is still possible that URO-synthase could bind to the nascent linear tri- or tetra-pyrrole HMB-synthase/substrate intermediates directly, although 3D structure studies of HMB-synthase indicated that the dipyrrole cofactor, and perhaps the enzyme-substrate intermediates, are buried in the structure.[47–49] Since the *in vitro* concentrations of these cytosolic heme biosynthetic enzymes were at least 150-fold higher than those in liver,[50] it is unlikely that these proteins bind each other even weakly *in vivo*. On the other hand, these studies do not rule out the possibility of a transient *in vivo* complex, possibly mediated by other proteins serving as a scaffold.[51]

The NMR perturbation studies reported here mapped the URO-synthase active site to a specific region of the inter-domain cleft by identifying residues whose resonances were strongly perturbed when the isotopically-labeled enzyme was titrated with either its cyclic tetrapyrrole product, URO'gen III, or the linear tetrapyrrole substrate analogue, NMF-bilane (see Fig. 8). Additionally, weak to moderate resonance perturbations were observed for buried residues that were in close spatial contact, but otherwise distant in the primary structure, indicating that additional minor conformational changes in the enzyme's interior and hinge region occurred upon ligand binding. Additional evidence in support of the URO-synthase active site residues identified by perturbation mapping included (1) the occurrence of strongly perturbed putative active site residues within clusters of perturbed residues, (2) the congruent *in silico* docking predictions for both URO'gen III and NMF-bilane, (3) the active sites' positive electrostatic surface charge, which presumably enables steering of the negatively-charged substrate to this site, and (4), the high degree of conservation of the predicted active site residues among 13 eukaryotic URO-synthases (including mammalian, murine, avian, reptilian, piscine, invertebrate and yeast sequences). Thus, within each cluster, the residues that were the most perturbed, at the cleft surface, most conserved, and necessary for enzymatic activity would be the best candidates for contact residues. As detailed below, these four lines of corroborating evidence identified certain residues that likely comprise the active site.

Notably, L6/K7/D8, Y19/I20, I33/V35/L36, T62/S63/R65, G100/T103, R148, V171, F196/S197, A229/R230, and L251 were the most perturbed residues in their respective clusters identified by titration with both ligands. These clusters of perturbed residues presumably represent active site contact regions. Moreover, surface residues D8, Y19, L36, R65. R148, F196, and S197, were highly likely contact residues in the crystal structure model, since they were both the most perturbed residues within their clusters and were within 4 Å of both the docked URO'gen III and NMF-bilane ligands.

In addition, the positively-charged residues K7, R65, and R148 were major contributors to the overall positive charge of the active site and all three were perturbed by both negatively-charged ligands. Although the electrostatic surface potential of URO-synthase was mostly negative, the cleft region was highly positively-charged, which would presumably favor steering of the ligands to sites experimentally determined by NMR perturbation studies.

Finally, it is significant that surface residues in the cleft region perturbed by one or both ligands were highly conserved ($\geq$92%) in 13 eukaryotes, including yeast. These highly-conserved and perturbed residues included K7, Y19, L36, R65, G100, T103, Y168, F196, S197, G200, and L251. Of these, Matthews *et al.*[14] site-specifically mutated three and found reduced enzymatic activity for two, R65 and Y168 (74 and 49% of wild-type, respectively). In addition, mutagenesis of the highly-conserved T228 reduced the enzyme's activity to 32% of wild type. Although the T228 backbone amide could not be assigned by NMR, the adjacent subsurface residue, A229, was strongly perturbed by both ligands supporting a possible role for T228 as an active site residue. Since the HMB substrate of URO-synthase nonenzymatically autocatalyzes its own ring closure without D-ring isomerization resulting in URO'gen I, the primary function of the enzyme may be to stereoelectronically direct and stabilize the transition state leading to formation of the III-isomer. Thus, it is unlikely that any single residue will be found absolutely essential for catalytic activity, as previously suggested.[14]

A possible model of ligand binding is proposed in Figure 10 that shows the predicted docking of the lowest energy conformer of URO'gen III to the active site composed of the conserved, perturbed, surface residues. The teal-colored perturbed residues were >92% conserved in eukaryotes, while the sand-colored perturbed residues D8 and R148 were 62 and 54% conserved, respectively. It should be noted, however, that for large ligands, some active site residues may be less- or nonconserved, yet involved in catalysis or binding.[52,53] Although most of the domain 1 contact residues predicted by docking were also perturbed by ligand binding, there were additional perturbed cleft-surface residues in domain 2 (e.g., G100, T103, and E123), indicating that the tetrapyrroles also bound to this upper region of the cleft. Although Figure 10 provides a possible model of the binding of URO'gen III to the active site identified by *in silico* docking and by chemical shift perturbation mapping, changes in positions of the tetrapyrrole acidic side chains may be possible, along with alterations in the angle of the ring within the cleft depending on cleft size. An NMR-derived solution structure may permit optimized docking and dynamic energy minimization studies to refine the present model.

In sum, these NMR studies established the nearly complete backbone and 85% side-chain resonance assignments for human URO-synthase and experimentally

mapped its active site in the cleft between domains 1 and 2, identifying putative contact residues involved in the binding of its substrate and product. In addition, these NMR studies of the interaction of URO-synthase with HMB-synthase or URO-decarboxylase did not support the long-held hypothesis that the cytosolic heme biosynthetic enzymes formed a protein-protein complex for efficient metabolism of ALA to coproporphyrinogen III.

ACKNOWLEDGMENTS

We thank Dr. Troy Burke for the design of the URO-synthase expression construct and for optimization of the purification of recombinant URO-synthase. Computational resources were provided by the Mount Sinai School of Medicine's Computational Biology Shared Research Facility.

REFERENCES

1. Anderson KE, Sassa S, Bishop DF, Desnick RJ. Disorders of heme biosynthesis: X-Linked sideroblastic anemia and the porphyrias. In: Scriver CR, Beaudet AL, Sly WS, Valle D, editors. The metabolic and molecular bases of inherited disease, 8th ed., Vol. 2. New York: McGraw-Hill; 2001. pp 2991–3062.
2. Tsai SF, Bishop DF, Desnick RJ. Human uroporphyrinogen III synthase: molecular cloning, nucleotide sequence, and expression of a full-length cDNA. Proc Natl Acad Sci USA 1988;85:7049–7053.
3. Aizencang G, Solis C, Bishop DF, Warner C, Desnick RJ. Human uroporphyrinogen-III synthase: genomic organization, alternative promoters, and erythroid-specific expression. Genomics 2000;70: 223–231.
4. Astrin KH, Warner CA, Yoo HW, Goodfellow PJ, Tsai SF, Desnick RJ. Regional assignment of the human uroporphyrinogen III synthase (UROS) gene to chromosome 10q25.2 Øq26.3. Hum Genet 1991;87:18–22.
5. Tsai SF, Bishop DF, Desnick RJ. Purification and properties of uroporphyrinogen III synthase from human erythrocytes. J Biol Chem 1987;262:1268–1273.
6. Omata Y, Sakamoto H, Higashimoto Y, Hayashi S, Noguchi M. Purification and characterization of human uroporphyrinogen III synthase expressed in *Escherichia coli*. J Biochem (Tokyo) 2004;136: 211–220.
7. Bogorad L. The enzymatic synthesis of porphyrins from porphobilinogen. I. Uroporphyrin I. J Biol Chem 1958;233:501–509.
8. Bogorad L. The enzymatic synthesis of porphyrins from porphobilinogen. II. Uroporphyrin III. J Biol Chem 1958;233:510–515.
9. Frydman RB, Feinstein G. Studies on porphobilinogen deaminase and uroporphyrinogen 3 cosynthase from human erythrocytes. Biochim Biophys Acta 1974;350:358–373.
10. Higuchi M, Bogorad L. The purification and properties of uroporphyrinogen I synthases and uroporphyrinogen III cosynthase. Interactions between the enzymes. Ann N Y Acad Sci 1975;244:401–418.
11. Sancovich HA, Battle AM, Grinstein M. Porphyrin biosynthesis. VI. Separation and purification of porphobilinogen deaminase and uroporphyrinogen isomerase from cow liver porphobilinogenase an allosteric enzyme. Biochim Biophys Acta 1969;191:130–143.
12. Battersby AR, Fookes CJR, Matcham GW, McDonald E, Gustafson-Potter KE. Biosynthesis of the natural porphyrins: experiments on the ring-losure steps and with the hydroxy-analogue of porphobilinogen. J Chem Soc Chem Commun 1979:316–319.
13. Tsai SF, Bishop DF, Desnick RJ. Coupled-enzyme and direct assays for uroporphyrinogen III synthase activity in human erythrocytes and cultured lymphoblasts. Enzymatic diagnosis of heterozygotes and homozygotes with congenital erythropoietic porphyria. Anal Biochem 1987;166:120–133.
14. Mathews MA, Schubert HL, Whitby FG, Alexander KJ, Schadick K, Bergonia HA, Phillips JD, Hill CP. Crystal structure of human uroporphyrinogen III synthase. EMBO J 2001;20:5832–5839.
15. Anderson PM, Desnick RJ. Purification and properties of delta-aminolevulinate dehydrase from human erythrocytes. J Biol Chem 1979;254:6924–6930.
16. Gill SC, von Hippel PH. Calculation of protein extinction coefficients from amino acid sequence data. Anal Biochem 1989;182:319–326.
17. Anderson PM, Desnick RJ. Purification and properties of uroporphyrinogen I synthase from human erythrocytes. Identification of stable enzyme-substrate intermediates. J Biol Chem 1980;255:1993–1999.
18. Straka JG, Kushner JP, Pryor MA. Uroporphyrinogen decarboxylase. A method for measuring enzyme activity. Enzyme 1982;28:170–185.
19. Malakhov MP, Mattern MR, Malakhova OA, Drinker M, Weeks SD, Butt TR. SUMO fusions and SUMO-specific protease for efficient expression and purification of proteins. J Struct Funct Genomics 2004;5:75–86.
20. Mossessova E, Lima CD. Ulp1-SUMO crystal structure and genetic analysis reveal conserved interactions and a regulatory element essential for cell growth in yeast. Mol Cell 2000;5:865–876.
21. Medek A, Olejniczak ET, Meadows RP, Fesik SW. An approach for high-throughput structure determination of proteins by NMR spectroscopy. J Biomol NMR 2000;18:229–238.
22. Tugarinov V, Kay LE. Ile, Leu, and Val methyl assignments of the 723-residue malate synthase G using a new labeling strategy and novel NMR methods. J Am Chem Soc 2003;125:13868–13878.
23. Pichon C, Atshaves BP, Xue T, Stolowich NJ, Scott AI. Studies on URO'gen III sythase with modified bilanes. Bioorg Med Chem Lett 1994;4:1105–1110.
24. Delaglio F, Grzesiek S, Vuister GW, Zhu G, Pfeifer J, Bax A. NMRPipe: a multidimensional spectral processing system based on UNIX pipes. J Biomol NMR 1995;6:277–293.
25. Johnson BA, Blevins RA. NMR view: a computer program for the visualization and analysis of NMR data. J Biomol NMR 1994;4:603–614.
26. Yamazaki T, Lee W, Arrowsmith CH, Mahandiram DR, Kay LE. A suite of triple resonance NMR experiments for the backbone assignment of 15N, 13C, 2H labeled proteins with high sensitivity. J Am Chem Soc 1994;116:11655–11666.
27. Logan TM, Zhou MM, Nettesheim DG, Meadows RP, Van Etten RL, Fesik SW. Solution structure of a low molecular weight protein tyrosine phosphatase. Biochemistry 1994;33:11087–11096.
28. Goto NK, Gardner KH, Mueller GA, Willis RC, Kay LE. A robust and cost-effective method for the production of Val. Leu Ile (delta 1) methyl-protonated 15N-, 13C-, 2H-labeled proteins. J Biomol NMR 1999;13:369–374.
29. Neri D, Szyperski T, Otting G, Senn H, Wuthrich K. Stereospecific nuclear magnetic resonance assignments of the methyl groups of valine and leucine in the DNA-binding domain of the 434 repressor by biosynthetically directed fractional 13C labeling. Biochemistry 1989;28:7510–7516.
30. Morris GM, Goodsell DS, Halliday RS, Huey R, Hart WE, Belew RK, Olson AJ. Automated docking using a Lamarckian genetic algorithm and an empirical binding free energy function. J Comput Chem 1998;19:1639–1662.
31. MacKerell AD, Jr, Bashford D, Bellot M, Dunbrack RLJDE, Field MJ, Fischer S, Gao J, Guo H, Ha S, Joseph-McCarthy D, Kuchnir L, Kuczera K, Lau FTK, Mattos C, Michnick S, Ngo T, Nguyen DT, Prodhom B, Reiher WEI, Roux B, Schlenkrich B, Smith J, Stote R, Straub S, Watanabe M, Wiorkiewicz-Kuczera J, Karplus M. All-atom empirical potential for molecular modeling and dynamics studies of proteins. J Phys Chem B 1998;102:3586–3616.
32. Dewar JS, Zoebisch EG, Healy EF, Stewart JJP. AM1: a new general purpose quantum mechanical molecular model J Am Chem Soc 1985;107:3902–3909.

33. Frisch MJ, Trucks GW, Schlegel HB, Scuseria GE, Robb MA, Cheeseman JR, Zakarzewsky VG, Montgomery JA, Stratman RE, Burant JC, Dapprich S, Millam JC, Daniels AD, Kudin KN, Strain MC, Farkas O, Tomasi J, Barone V, Cossi M, Cammi R, Menucci B, Pomelli C, Adamo C, Clifford S, Ochterski J, Petersson GA, Ayala PY, Cui Q, Morokuma K, Malick DK, Rabuck AD, Raghavachari K, Foresman JB, Ciolowski J, Ortiz JV, Stefanov BB, Liu G, Liashenko A, Piskorz P, Komaromi I, Gomperts R, Martin RL, Fox DJ, Keith T, Al-Laham MA, Peng CY, Nanayakkara A, Gonzales C, Challacombe M, Gill PMW, Johnson BG, Chen W, Wong MW, Andres JL, Head-Gordon M, Replogle ES, Pople JA. Gaussian-98, Revision A. 1. Pittsburg, PA: Gaussian; 1998.
34. Cavanagh J, Fairbrother WJ, Palmer AGI, Skelton NJ. Protein NMR spectroscopy. Principles and practice. New York: Academic Press; 1996. p 587.
35. Katoh E, Louis JM, Yamazaki T, Gronenborn AM, Torchia DA, Ishima R. A solution NMR study of the binding kinetics and the internal dynamics of an HIV-1 protease-substrate complex. Protein Sci 2003;12:1376–1385.
36. Roberts AG, Elder GH. Purification and properties of uroporphyrinogen decarboxylase from human erythrocytes. Methods Enzymol 1997;281:349–355.
37. Alwan AF, Mgbeje BI, Jordan PM. Purification and properties of uroporphyrinogen III synthase (cosynthase) from an overproducing recombinant strain of *Escherichia coli* K-12. Biochem J 1989;264: 397–402.
38. Seavey BR, Farr EA, Westler WM, Markley JL. A relational database for sequence-specific protein NMR data. J Biomol NMR 1991;1:217–236.
39. Wishart DS, Sykes BD, Richards FM. The chemical shift index: a fast and simple method for the assignment of protein secondary structure through NMR spectroscopy. Biochemistry 1992;31:1647–1651.
40. Wishart DS, Sykes BD. The 13C chemical-shift index: a simple method for the identification of protein secondary structure using 13C chemical-shift data. J Biomol NMR 1994;4:171–180.
41. Kabsch W, Sander C. Dictionary of protein secondary structure: pattern recognition of hydrogen-bonded and geometrical features. Biopolymers 1983;22:2577–2637.
42. Jordan PM, Warren MJ. Evidence for a dipyrromethane cofactor at the catalytic site of E. coli porphobilinogen deaminase. FEBS Lett 1987;225:87–92.
43. Warren MJ, Jordan PM. Investigation into the nature of substrate binding to the dipyrromethane cofactor of *Escherichia coli* porphobilinogen deaminase. Biochemistry 1988;27:9020–9030.
44. DeLano WL. The Pymol molecular graphics system. San Carlos, CA: DeLano Scientific; 2002.
45. Hart GJ, Battersby AR. Purification and properties of uroporphyrinogen III synthase (co-synthetase) from *Euglena gracilis*. Biochem J 1985;232:151–160.
46. Baker NA, Sept D, Joseph S, Holst MJ, McCammon JA. Electrostatics of nanosystems: application to microtubules and the ribosome. Proc Natl Acad Sci USA 2001;98:10037–10041.
47. Louie GV, Brownlie PD, Lambert R, Cooper JB, Blundell TL, Wood SP, Warren MJ, Woodcock SC, Jordan PM. Structure of porphobilinogen deaminase reveals a flexible multidomain polymerase with a single catalytic site. Nature 1992;359:33–39.
48. Helliwell JR, Nieh Y-P, Raftery J, Cassetta A, Habash J, Carr PD, Ursby T, Wulff M, Thompson AW, Niemann AC, Hädner A. Time-resolved structures of hydroxymethylbilane synthase (Lys59Gln mutant) as it is loaded with substrate in the crystal determined by Laue diffraction. J Chem Soc Faraday Trans 1998;94:2615–2622.
49. Helliwell JR, Nieh YP, Habash J, Fauldner PF, Raftery J, Cianci M, Wulff M, Hädner A. Time-resolved and static-ensemble structural chemistry of hydroxymethylbilane synthase. Faraday Discuss 2002;122:131–144.
50. Bishop DF, Desnick RJ. Assays of the heme biosynthetic enzymes. Preface Enzyme 1982;28:91–93.
51. Langeberg LK, Scott JD. A-kinase-anchoring proteins. J Cell Sci 2005;118:3217–3220.
52. El-Kabbani O, Old SE, Ginell SL, Carper DA. Aldose and aldehyde reductases: structure-function studies on the coenzyme and inhibitor-binding sites. Mol Vis 1999;5:20.
53. Lala A, Gwinn M, De Nardin E. Human formyl peptide receptor function role of conserved and nonconserved charged residues. Eur J Biochem 1999;264:495–499.